Chapter 19

4D Seismic

Martin Landrø

19.1 Introduction

The term 4D seismic reflects that calendar time represents the fourth dimension. A more precise term is *repeated seismic*, because that is actually what is done: a seismic survey over a given area (oil/gas field) is repeated in order to monitor production changes. *Time-lapse seismic* is another term used for this. For some reason, the term 4D seismic is most common, and we will therefore use it here. It is important to note that if we repeat 2D surveys, it is still denoted 4D seismic according to this definition. Recent examples of such surveys are repeated 2D lines acquired over the Troll gas province.

Currently there are three major areas where 4D seismic is applied. Firstly, to monitor changes in a producing hydrocarbon reservoir. This is now an established procedure being used worldwide. So far, 4D seismic has almost exclusively been used for clastic reservoirs and only rarely for carbonate reservoirs. This is because carbonate reservoirs (apart from those in porous chalk) are stiffer, and the effect on the seismic parameters of substituting oil with water is far less pronounced. Secondly, 4D seismic is being used to monitor underground storage of CO_2. Presently, there is a global initiative to decrease the atmospheric CO_2 content, and one way to achieve this goal is to pump huge amounts of CO_2 into saline aquifers. A third application of 4D seismic (with other geophysical methods) is the monitoring of geohazards (landslides, volcanoes etc.), however this will not be covered here.

M. Landrø (✉)
NTNU Trondheim, Trondheim, Norway
e-mail: martin.landro@ntnu.no

The business advantage of using 4D seismic on a given field is closely correlated with the complexity of the field. Figure 19.1 shows a 3D perspective view of the top reservoir (top Brent) interface for the Gullfaks Field. Since the oil is trapped below such a complex 3D surface, it is not surprising that oil pockets can remain untouched even after 10–15 years of production. Since 4D seismic can be used to identify such pockets, it is easy to understand the commercial value of such a tool. However, if the reservoir geometry is simpler, the number of untapped hydrocarbon pockets will be less and the business benefit correspondingly lower.

The first 4D seismic surveys were probably acquired in America in the early 1980s. It was soon realised that heavy oil fields were excellent candidates for 4D seismic. Heavy oil is highly viscous, so thermal methods such as combustion or steam injection were used to increase its mobility. Combustion describes a burning process, which normally is maintained by injection of oxygen or air. As the reservoir is heated, the seismic P-wave velocity decreases, and this results in amplitude changes between baseline and monitor seismic surveys.

The best known example is maybe the one published by Greaves and Fulp in 1987, for which they received the award for the best paper in *Geophysics*. They showed that such thermal recovery methods could be monitored by repeating conventional 3D land seismic surveys (Fig. 19.2). These early examples of seismic monitoring of thermal recovery methods did not immediately lead to a boom in the 4D industry, mainly because they were performed on small and very shallow onshore fields. The major breakthrough for commercial 4D seismic surveys in the North Sea was the Gullfaks 4D study launched by Statoil in 1995. Together with WesternGeco a pilot study was done

K. Bjørlykke (ed.), *Petroleum Geoscience: From Sedimentary Environments to Rock Physics*,
DOI 10.1007/978-3-642-34132-8_19,

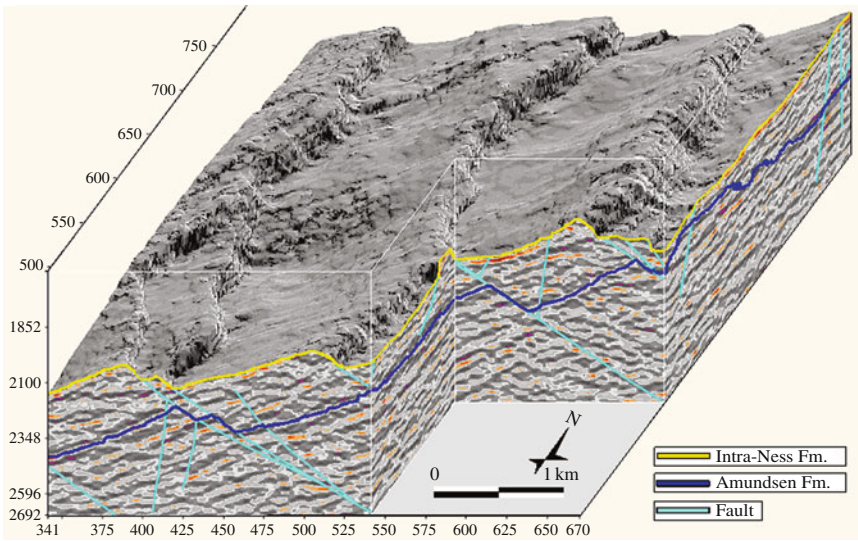

Fig. 19.1 3D seismic image of the top reservoir interface (top Brent Group) at the Gullfaks Field. Notice the fault pattern and the complexity of the reservoir geometry

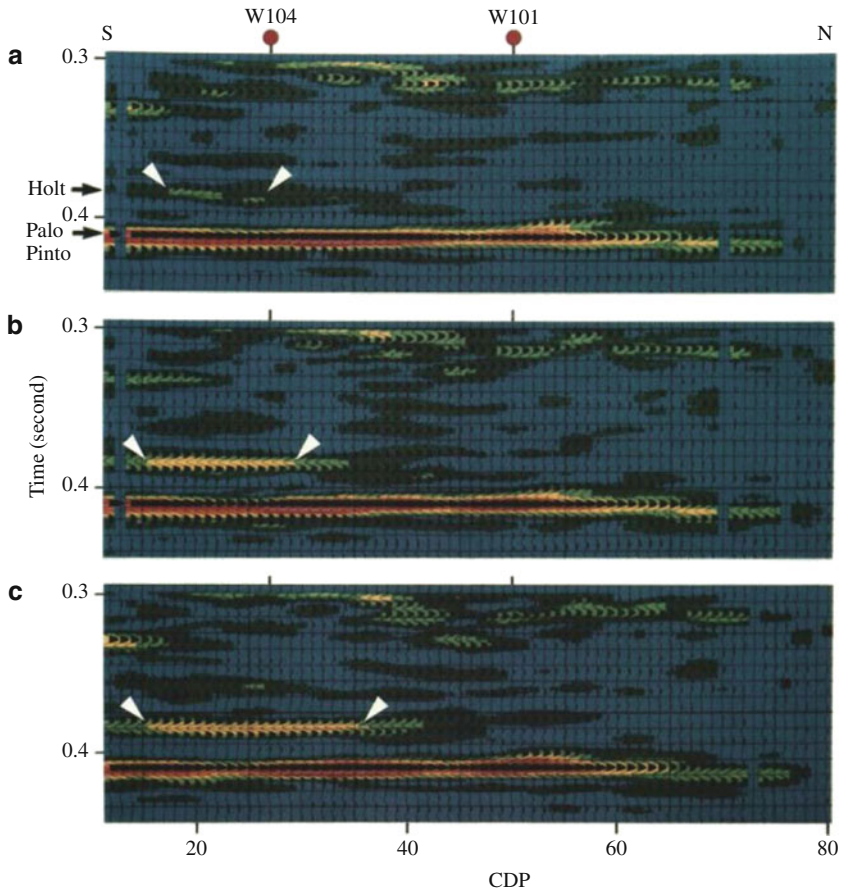

Fig. 19.2 Shows clear 4D amplitude brightening (*top* Holt horizon) as the reservoir is heated. Also note the extended area (marked by *white arrows*) for this amplitude increase. (Greaves and Fulp, Geophysics 52, 1987)

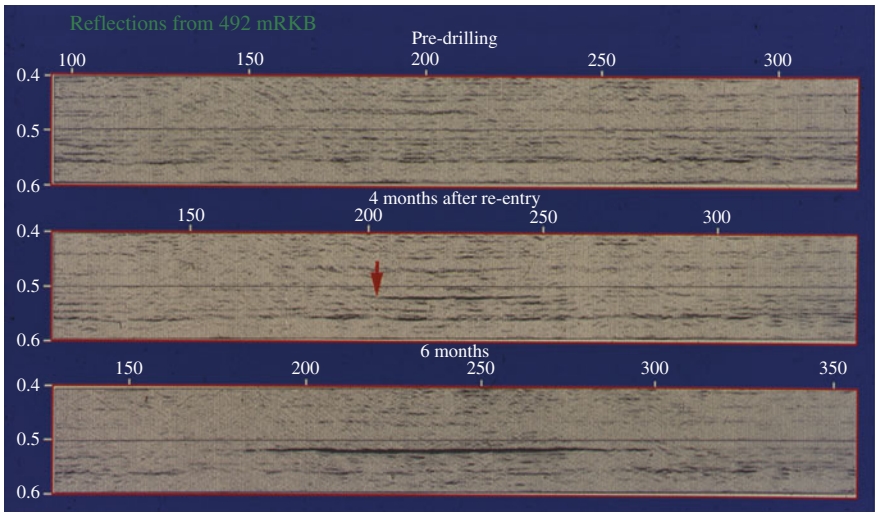

Fig. 19.3 Seismic monitoring of the underground flow caused by drilling a deep Jurassic well in 1989 in the North Sea. The new seismic event marked by the *red arrow* on the *middle section* is interpreted as a gas-filled sand body. On the *lower section* (6 months after the drilling event) the areal extent of this event has increased further. Figure provided by Dag O. Larsen, from his SEG-presentation in 1990

over the major northern part of the field, and the initial interpretation performed shortly after this monitor survey demonstrated a promising potential.

However, the first use of 4D seismic in the North Sea was probably the monitoring of an underground flow (Larsen and Lie 1990). In January 1989, when drilling a deep Jurassic well (2/4-14), Saga Petroleum had to shut the well by activating the BOP. The rig was moved off location, and a relief well was spudded. When the rig was reconnected 3 months later, the pressure had dropped, indicating a subsurface fluid transfer. The flow and the temperature measurements indicated a leak in the casing at 1,334 mSS. A strong amplitude increase at the top of a sand layer could be observed on the time-lapse seismic data close to this well (Fig. 19.3) – showing the fluid was gas.

The areal extent of this 4D anomaly increased from one survey to the next. After 4 months this amplitude increase was also observed on shallower interfaces, probably connected to gas migrating upwards to shallower sand layers.

19.2 Rock Physics and 4D Seismic

When a hydrocarbon field is produced, there are several reservoir parameters that might change, most crucially:
- fluid saturation changes
- pore pressure changes
- temperature changes

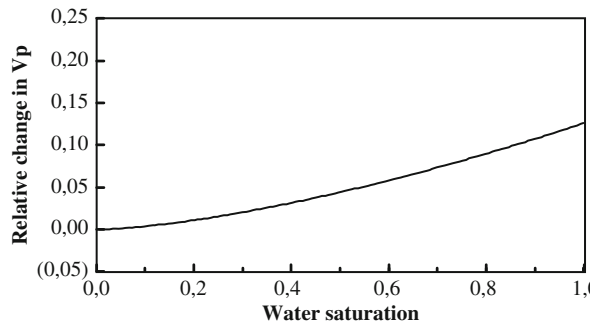

Fig. 19.4 Relative change in P-wave velocity versus water saturation, estimated from a calibrated Gassmann model. Zero water saturation corresponds to 100% oil

- changes in layer thickness (compaction or stretching).

A critical part of all 4D studies is to link key reservoir parameters like pore pressure and fluid saturation to the seismic parameters. Rock physics provides this link. Both theoretical rock physics models and laboratory experiments are used as important input to time-lapse seismic analysis. A standard way of relating for instance P-wave seismic velocity to changes in fluid saturation is to use the Gassmann model. Figure 19.4 shows one example, where a calibrated Gassmann model has been used to determine how the P-wave velocity changes with water saturation (assuming that the reservoir fluid is a mixture of oil and water).

In addition, various contact models have been proposed to estimate the effective modulus of a rock. Mavko, Mukerji and Dvorkin present some of these models in their rock physics handbook (1998). The Hertz-Mindlin model (Mindlin 1949) can be used to describe the properties of pre-compacted granular rocks. The effective bulk modulus of dry random identical sphere packing is given by:

$$K_{\text{eff}} = \left\{ \frac{C_p^2(1-\varphi^2)G^2P}{18\pi^2(1-\sigma)^2} \right\}^{\frac{1}{3}} \tag{19.1}$$

where C_{p} is the number of contact points per grain, φ is porosity, G is the shear modulus of the solid grains, σ is the Poisson ratio of the solid grains and P is the effective pressure (that is $P = P_{\text{eff}}$). The shear modulus is given as:

$$G_{\text{eff}} = \left\{ \frac{3C_{\text{p}}^2(1-\varphi)^2G^2P}{2\pi^2(1-\sigma)^2} \right\}^{\frac{1}{3}} \frac{5-4\sigma}{5(2-\sigma)} \tag{19.2}$$

This leads to:

$$V_{\text{P}} = \sqrt{\frac{K_{\text{eff}} + \frac{4}{3}G_{\text{eff}}}{\rho}} \tag{19.3}$$

$$V_{\text{S}} = \sqrt{\frac{G_{\text{eff}}}{\rho}} \tag{19.4}$$

where V_{p} and V_{s} are P- and S-wave velocities, respectively, and ρ is the sandstone density. Inserting Eqs. (19.1) and (19.2) into Eqs. (19.3) and (19.4) and computing the $V_{\text{p}}/V_{\text{s}}$ ratio, yields (assuming $\sigma = 0$):

$$\frac{V_{\text{P}}}{V_{\text{S}}} = \sqrt{2}. \tag{19.5}$$

This means that according to the simplest granular model (Hertz-Mindlin), the $V_{\text{p}}/V_{\text{s}}$ ratio should be constant as a function of confining pressure if we assume the rock is dry. The Hertz-Mindlin model assumes the sand grains are spherical and that there is a certain area of grain-to-grain contacts. A major shortcoming of the model is that at the limit of unconsolidated sands, both the P- and S-wave velocities will have the same behaviour with respect to pressure changes, as shown in Eq. (19.5). Combining with the Gassmann (1951) model (i.e. introducing fluids in the pore system of the rock), will ensure that the P-wave velocity approaches the fluid velocity for zero effective stress, and not zero as in the Hertz-Mindlin model (dry rock assumption).

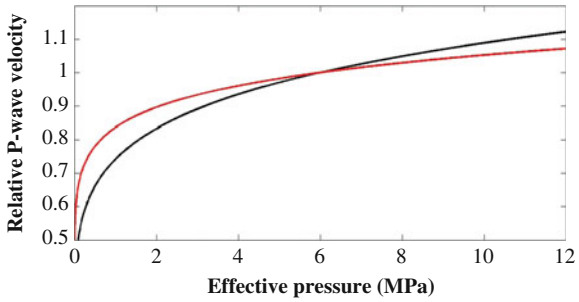

Fig. 19.5 Typical changes in P-wave velocity versus effective pressure using the Hertz-Mindlin model. In this case the *in situ* effective pressure (prior to production) is 6 MPa, and we see that a decrease in effective pressure leads to a decrease in P-wave velocity. The *black curve* represents the Hertz-Mindlin model (exponent = 1/6, as in Eq. (19.6)), the *red curve* is a modified version of the Hertz-Mindlin model (exponent = 1/10) that better fits the ultrasonic core measurements

If we assume that the *in situ* (base survey) effective pressure is P_0 we see from Eq. (19.3) that the relative P-wave velocity versus effective pressure is given as:

$$\frac{V_{\text{P}}}{V_{P_0}} = \left(\frac{P}{P_0}\right)^{\frac{1}{6}} \tag{19.6}$$

Figure 19.5 shows this relation for an *in situ* effective pressure of 6 MPa. When such curves are compared to ultrasonic core measurements, the slope of the measured curve is generally smaller than this simple theoretical curve. The cause for this might be multifold: Firstly, the Hertz-Mindlin model assumes the sediment grains are perfect, identical spheres, which is never found in real samples. Secondly, the ultrasonic measurements might suffer from scaling issues, core damage and so on. Thirdly, cementation effects are not included in the Hertz-Mindlin model. It is therefore important to note that there are major uncertainties regarding the actual dependency between seismic velocity and pore pressure changes.

19.3 Some 4D Analysis Techniques

The analysis of 4D seismic data can be divided into two main categories, one based on the detection of amplitude changes, the other on detecting travel-time

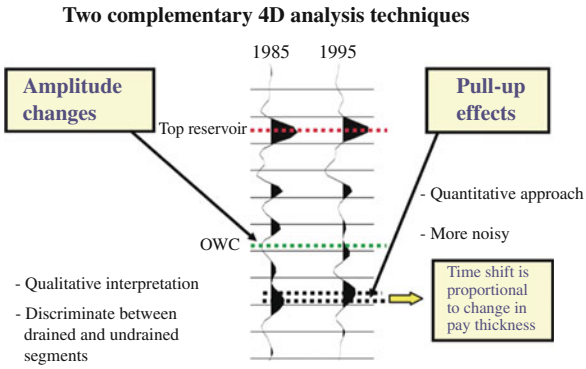

Fig. 19.6 Shows the two 4D analysis techniques. Notice there are no amplitude changes at top reservoir between 1985 and 1995, but huge amplitude changes at the oil/water contact (OWC). Also note the change in travel time (marked by the *yellow arrow*) for the seismic event below the oil/water contact

changes, see Fig. 19.6. Practical experience has shown that the amplitude method is most robust, and therefore this has been the most frequently employed method. However, as the accuracy of 4D seismic has improved, the use of accurate measurements of small timeshifts is increasingly the method of choice. There are several examples where the timeshift between two seismic traces can be determined with an accuracy of a fraction of a millisecond. A very attractive feature of 4D timeshift measurement is that it is proportional to the change in pay thickness, and this method provides a direct quantitative result. The two techniques are complementary in that amplitude measurement is a local feature (measuring changes close to an interface), while the timeshift method measures average changes over a layer, or even a sequence of layers.

In addition to the direct methods mentioned above, 4D seismic interpretation is aided by seismic modelling of various production scenarios, often combined with reservoir fluid flow simulation and 1D scenario modelling based on well logs.

19.4 The Gullfaks 4D Seismic Study

One of the first commercially successful 4D examples from the North Sea was the Gullfaks study (Landrø et al. 1999). There are two simple explanations for this success: the complexity of the reservoir geometry (Fig. 19.1) means that there will be numerous pockets of undrained oil, and there is a strong correlation between the presence of oil and amplitude brightening as shown in Fig. 19.7.

In addition to these two observations, a rock physics feasibility study was done, and the main results are summarised in Fig. 19.8. It is important to note that the key parameter for 4D seismic is not the relative change in the seismic parameters, but the expected change in reflectivity between the base and monitor surveys. If we assume that the top reservoir interface separates the cap rock (Layer 1) and the reservoir (Layer 2), it is possible to estimate the relative change in the zero offset reflection coefficient (Landrø et al. 1999) caused by production changes in the reservoir layer. Denoting the acoustic impedances (velocity times density) in Layers 1 and 2 by λ_1 and λ_2, respectively, and using B and M to denote base and monitor surveys, we find that the change in reflectivity is given as (Landrø et al. 1999):

$$\frac{\Delta R}{R} = \frac{\lambda_2^M - \lambda_2^B}{\lambda_2^B - \lambda_1^B} = \frac{\Delta \mathrm{AI(production)}}{\Delta \mathrm{AI(original)}}. \qquad (19.7)$$

Here we have assumed that the change in acoustic impedance in Layer 2 is small compared to the actual impedance. Equation (19.7) means that the change in reflectivity is equal to the change in acoustic impedance in Layer 2 divided by the original (pre-production) acoustic impedance contrast between Layers 1 and 2. For Gullfaks, the expected change in acoustic impedance is 8% (assuming 60% saturation change, Fig. 19.8) while the original acoustic impedance contrast for top reservoir was approximately 18%. The estimated relative change in reflectivity is therefore 44% (8/18). This is the basic background for the success of using 4D seismic at Gullfaks, as shown in Fig. 19.9. The effect of replacing oil with water is evident on this figure, and is further strengthened by the amplitude difference map taken at the original oil-water contact (Fig. 19.10). Several Gullfaks wells have been drilled based on 4D interpretation, and a rough estimate of the extra income generated by using time-lapse seismic data is more than 1 billion USD.

19.5 Repeatability Issues

The quality of a 4D seismic dataset is dependent on several issues, such as reservoir complexity and the complexity of the overburden. However, the most important issue that we are able to influence is the

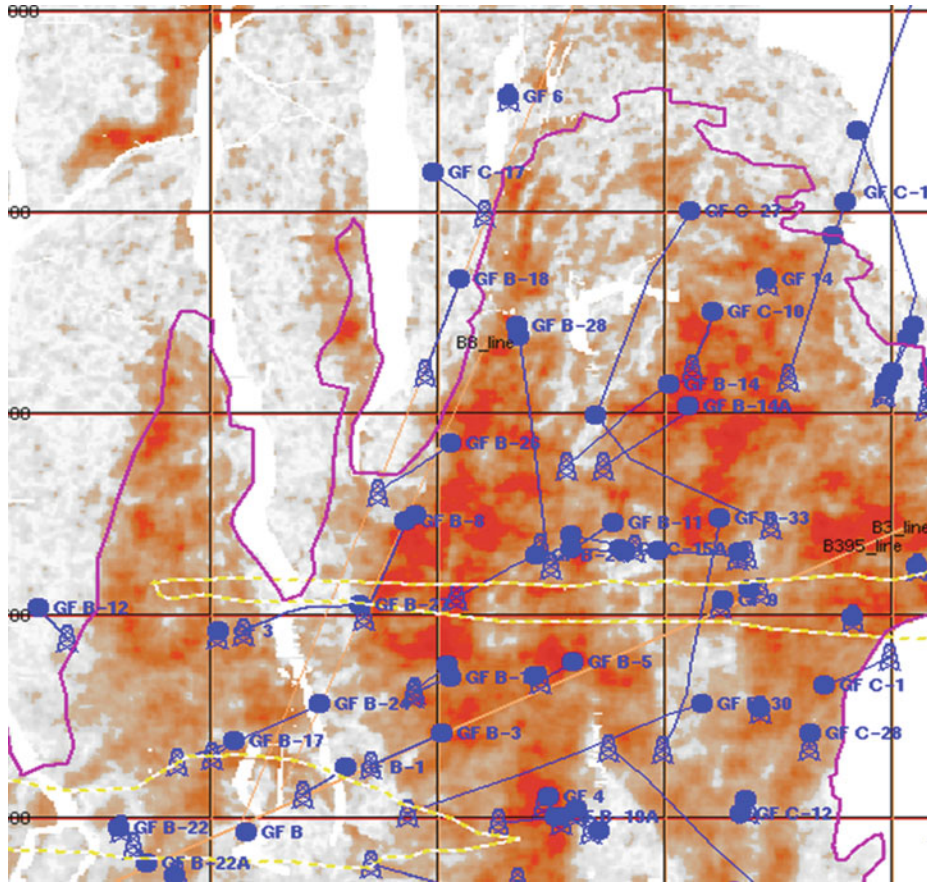

Fig. 19.7 Amplitude map for the top reservoir event at Gullfaks. The *purple solid line* represents the original oil-water contact. Notice the strong correlation between high amplitudes (*red colours*) and presence of oil. The size of one square is 1,250 by 1,250 m

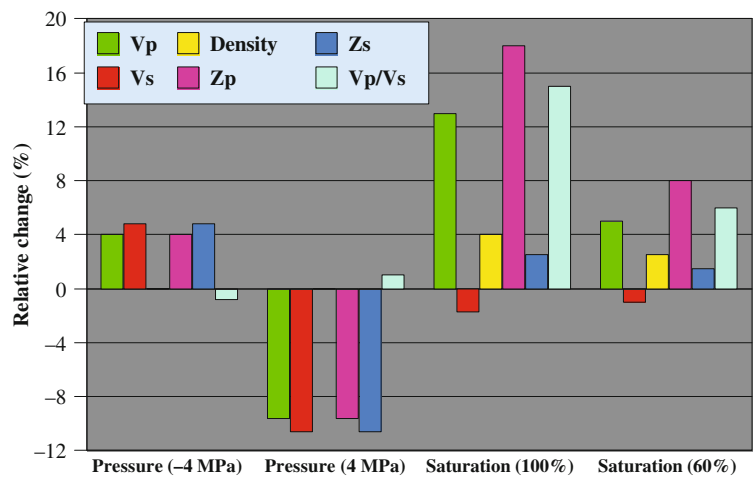

Fig. 19.8 Expected changes (based on rock physics) of key seismic parameters for pore pressure changes (*two left columns*) and for two fluid saturation scenario changes (*two right columns*)

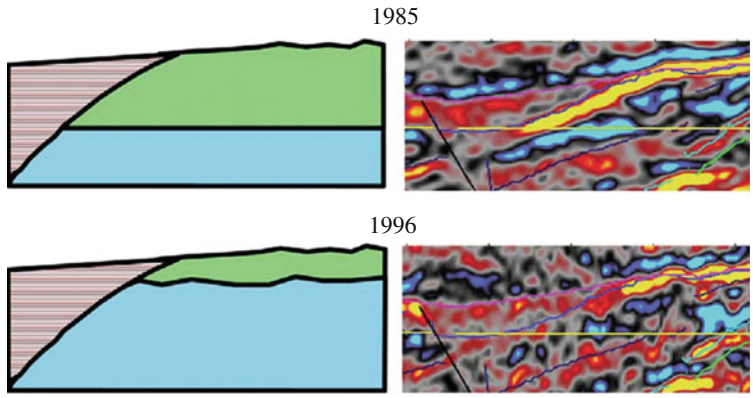

Fig. 19.9 Seismic data from 1985 (*upper right*) and 1996 (*lower right*) and the corresponding 4D interpretation to the *left* (*green* representing oil, and *blue* water)

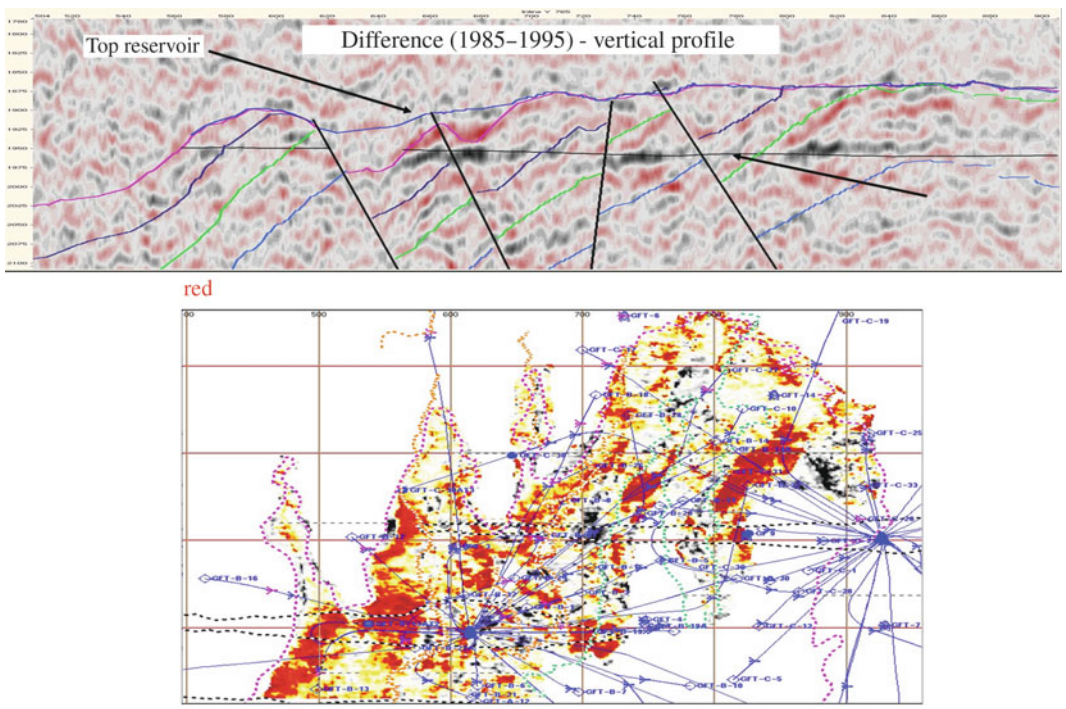

Fig. 19.10 Seismic difference section (*top*) and amplitude difference map at the original oil/water contact (OWC) (*bottom*). *Red colour* indicates areas that have been water-flushed, and *white areas* may represent bypassed oil

repeatability of the seismic data, i.e. how accurately we can repeat the seismic measurements. This *acquisition repeatability* is dependent on a number of factors such as:

- Varying source and receiver positions (x, y and z co-ordinates)
- Changing weather conditions during acquisition
- Varying seawater temperature
- Tidal effects
- Noise from other vessels or other activity in the area (rig noise)
- Varying source signal
- Changes in the acquisition system (new vessel, other cables, sources etc.)
- Variation in shot-generated noise (from previous shot).

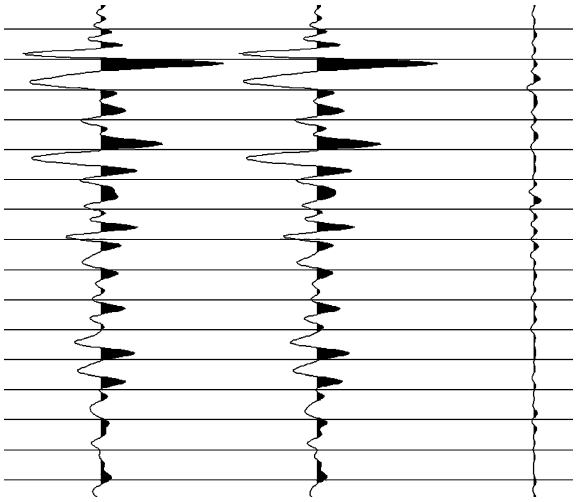

Fig. 19.11 Two VSP-traces measured at exactly the same position in the well, but with a slight difference in the source location (5 m in the *horizontal direction*). The distance between two timelines is 50 ms. The difference trace is shown to the right

Disregarding the weather conditions (the only way to "control" weather is to wait), most of the items listed are influenced by acquisition planning and performance. A common way to quantify repeatability is to use the normalised RMS (root-mean-square)-level, that is:

$$\mathrm{NRMS} = 2\frac{\mathrm{RMS(monitor - base)}}{\mathrm{RMS(monitor) + RMS(base)}}, \quad (19.8)$$

where the RMS-levels of the monitor and base traces are measured within a given time window. Normally, NRMS is measured in a time window where no production changes are expected. Figure 19.11 shows two seismic traces from a VSP (Vertical Seismic Profile) experiment where the receiver is fixed (in the well at approximately 2 km depth), and the source coordinates are changed by 5 m in the horizontal direction. We notice that the normalised rms-error (NRMS) in this case is low, only 8%.

In 1995 Norsk Hydro acquired a 3D VSP dataset over the Oseberg Field in the North Sea. This dataset consists of 10,000 shots acquired in a circular shooting pattern and recorded by a 5-level receiver string in the well. By comparing shot-pairs with different source positions (and the same receiver), it is possible to estimate the NRMS-level as a function of the horizontal distance between the shot locations. This is shown in Fig. 19.12, where approximately 70,000 shot pairs with varying horizontal mis-positioning are shown. The main message from this figure is clear. It is

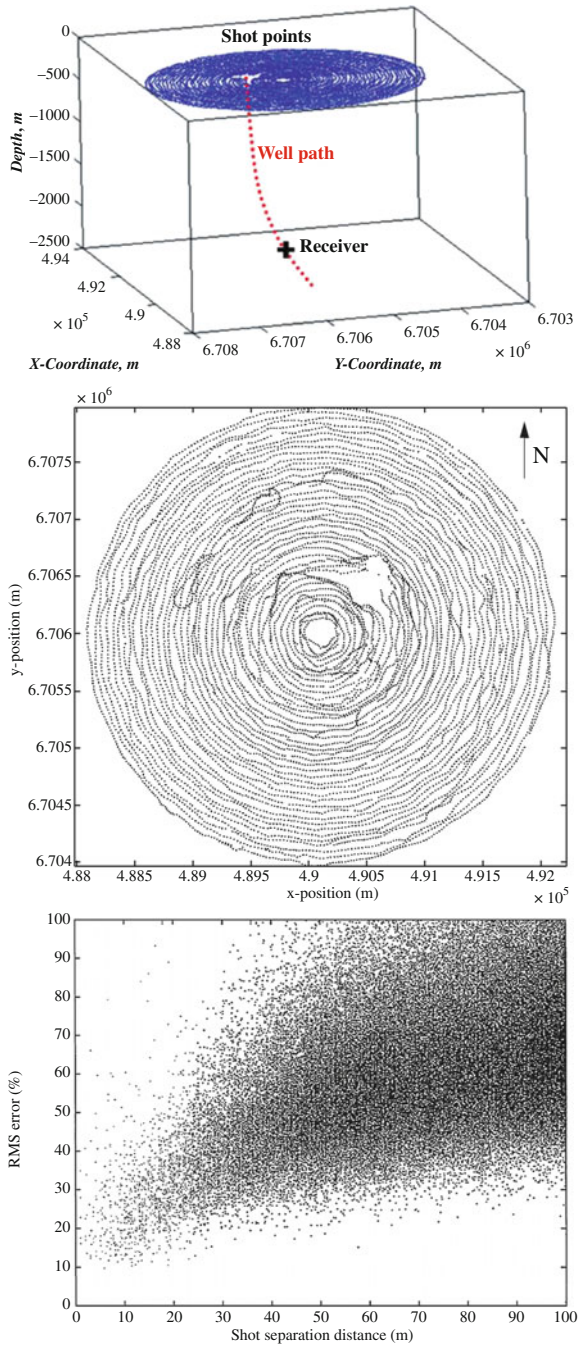

Fig. 19.12 *Top*: The 10,000 shot locations (map view) for the 3D VSP experiment over the Oseberg Field. *Bottom*: NRMS as a function of the source separation distance between approximately 70,000 shot pairs for the Oseberg 3D VSP dataset

important to repeat the horizontal positions both for sources and receivers as accurately as possible; even a misalignment of 20–30 m might significantly increase the NRMS-level.

Such a plot can serve as a variogram, since it shows the spread for each separation distance. Detailed studies have shown that the NRMS-level increases significantly in areas where the geology along the straight line between the source and receiver is complex. From Fig. 19.12 we see that the NRMS-value for a shot separation distance of 40 m might vary between 20 and 80% and a significant portion of this spread is attributed to variation in geology. This means that it is not straightforward to compare NRMS-levels between various fields, since the geological setting might be very different. Still, NRMS-levels are frequently used, since they provide a simple, quantitative measure. It is also important to note that the NRMS-level is frequency dependent, so the frequency band used in the data analysis should be given.

During the last two decades the focus on source and receiver positioning accuracy has lead to a significant improvement in the repeatability of 4D seismic data. Some of this is also attributed to better processing of time-lapse seismic data. This trend is sketched in Fig. 19.13. Today the global average NRMS-level is around 20–30%. It is expected that this trend will continue, though not at the same rate because the non-repeatable factors that need to be tackled to get beyond 20–30% are more difficult. In particular, rough weather conditions will represent a major hurdle.

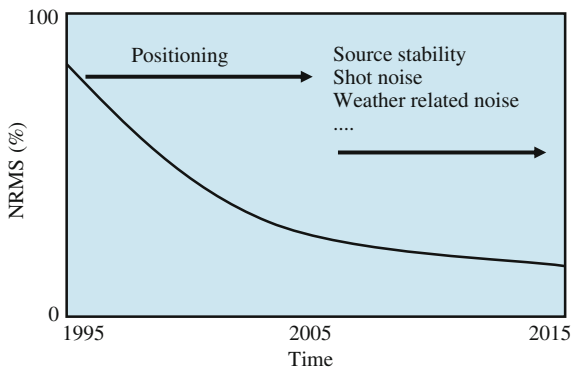

Fig. 19.13 Schematic view showing improvement in seismic repeatability (NRMS) versus calendar time

19.6 Fixed Receiver Cables

For marine seismic data, there are several ways to control the source and receiver positions. WesternGeco developed their Q-marine system, where the streamers can also be steered in the horizontal direction (x and y). This means that it is possible to repeat the receiver positions by steering the streamers into predefined positions. The devices are shown attached to the streamers in Fig. 19.14.

Another way to control the receiver positions is to bury the receiver cables on the seabed. One of the first commercial offshore surveys of this kind was launched at the Valhall Field in the southern part of the North Sea in 2003. Since then, more than 11 surveys have been acquired over this field. The buried

Fig. 19.14 Photographs of the birds (controlling devices) attached to a marine seismic cable at deployment (*left*) and in water operation (*right*). These devices make it possible to steer the cable with reasonable accuracy into a given position. (Courtesy of WesternGeco)

cables cover 70% of the entire field and the 4D seismic data quality is excellent. The fact that more than 10 surveys have been recorded into exactly the same receiver positions, opens for alternative and new ways (exploiting the multiplicity that more than 2 datasets offers) of analysing time-lapse seismic data. Other advantages offered by permanent receiver systems are:

- cheaper to increase the shot time interval in order to reduce the effect of shot generated noise
- continuous monitoring of background noise
- passive seismic
- possible to design a dedicated monitoring survey close to a problem well at short notice.

Despite all these advantages that permanent systems offer, there has not been a marked increase in such surveys so far, probably because of the relatively high upfront costs and the difficulty in quantifying in advance the extra value it would bring.

19.7 Geomechanical effects

Geomechanics has traditionally been an important discipline in both the exploration and production of hydrocarbons. However, the importance for geomechanics of time-lapse seismic monitoring was not fully realised before the first results from the chalk fields in the southern North Sea (Ekofisk and Valhall). Figure 19.15 shows map views of estimated travel-time shifts between base and monitor surveys at Ekofisk (Guilbot and Smith 2002), where the seafloor subsidence had been known for many years. The physical cause for the severe compaction of the chalk reservoir is twofold. Firstly, depletion of the field leads to pore-pressure decrease, and hence the reservoir rock compacts mechanically due to lack of pressure support. Secondly, the chemical reaction between the chalk matrix and the water replacing the oil leads to a weakening of the rock framework, allowing further compaction.

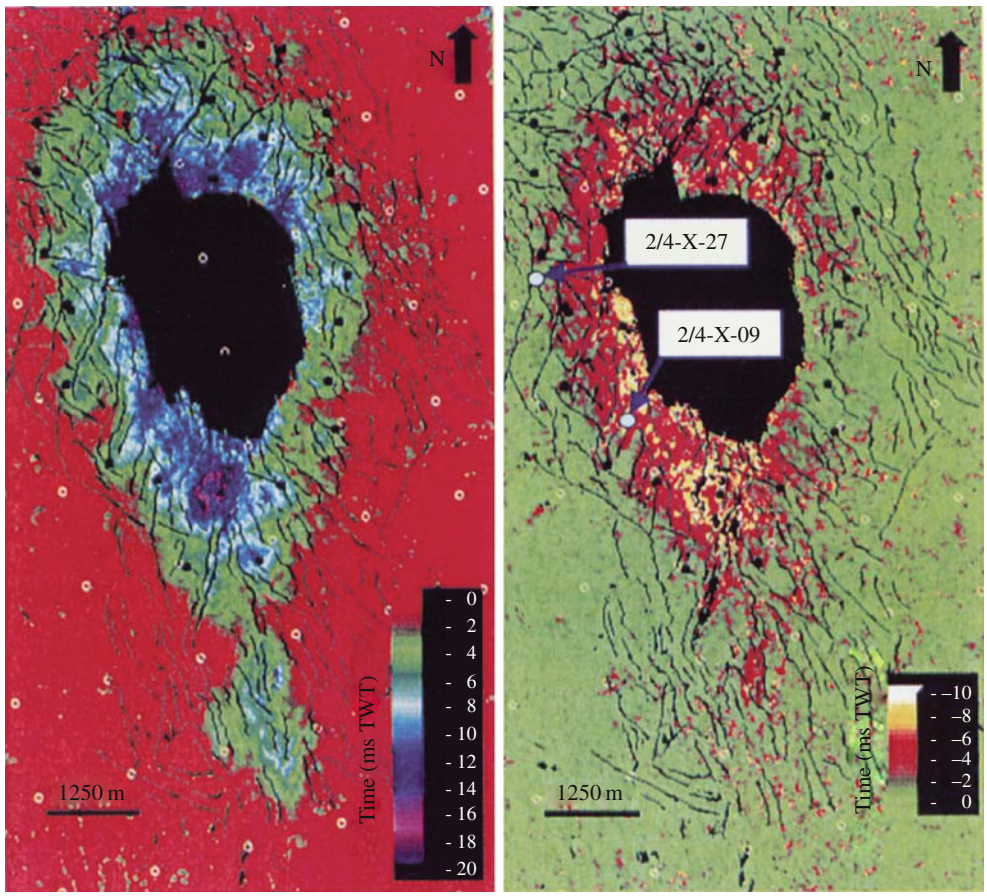

Fig. 19.15 4D timeshifts for top reservoir interface *(left)* and for the Ekofisk Formation *(right)*. The *black area* is caused by the gas chimney problem at Ekofisk, leading to lack of high quality seismic data in this area. (From Guilbot and Smith 2002)

When the reservoir rock compacts, the over- and underburden are stretched. This stretch is relatively small (of the order of 0.1%), However, this produces a small velocity decrease that is observable as timeshifts on time-lapse seismic data. Typical observations of seafloor subsidence show that the subsidence is less than the measured compaction for the reservoir. The vertical movement of the seafloor is typically less than that of the top reservoir (Settari 2002), though this is strongly dependent on reservoir geometry and the stiffness of the rocks above and below.

The most common way to interpret 4D seismic data from a compacting reservoir is to use geomechanical modelling as a complementary tool. One such example (Hatchell and Bourne 2005) is shown in Fig. 19.16. Note that the negative timeshifts (corresponding to a slowdown caused by overburden stretching) continue into the reservoir section. This is due to the fact that the reservoir section is fairly thin in this case and even a compaction of several metres is not sufficient to counteract the cumulative overburden effect. Similar effects have also been observed for sandstone reservoirs, such as the Elgin and Franklin fields. Normally, sandstone reservoirs compact less than chalk reservoirs and the corresponding 4D timeshifts are therefore less, but observable. Most of the North Sea sandstone reservoirs show negligible compaction, and therefore such effects are normally neglected in these 4D studies. However, as the accuracy of 4D seismic improves, this effect is expected to be observed at several of these fields as well. For instance the anticipated compaction of the Troll East field is around 0.5-1 m after 20 years of production, and this will probably be detectable by 4D seismic.

A major challenge when the thickness of subsurface layers is changed during production, is to distinguish between thickness changes and velocity changes. One way to resolve this ambiguity is to use geomechanical modelling as a constraining tool.

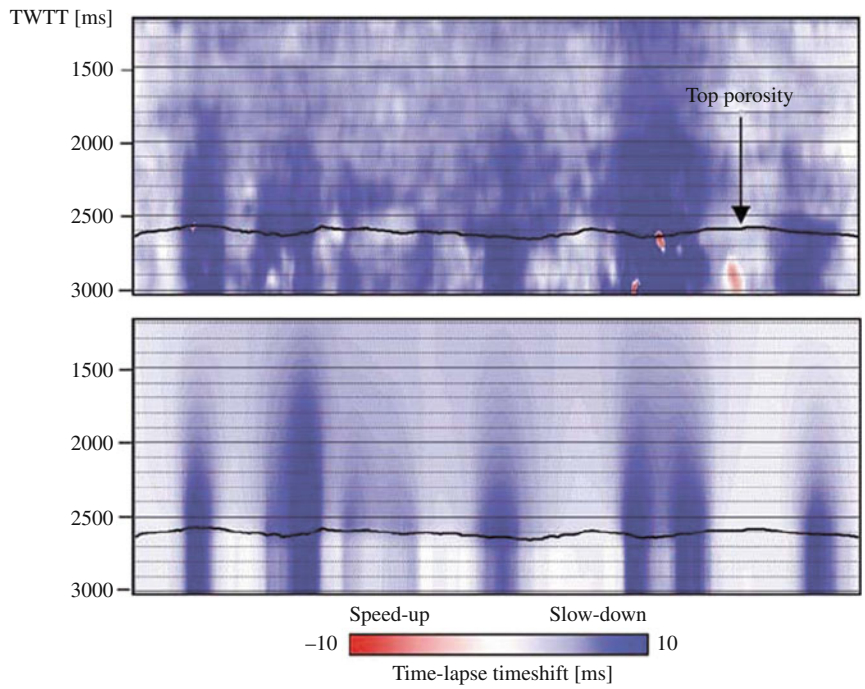

Fig. 19.16 Comparison of measured timeshifts from 4D seismic data (*top*) and geomechanical modelling. The *black solid line* represents top reservoir. Notice that the slowdown (*blue colours*) continues into the reservoir. (From Hatchell and Bourne 2005)

Another way is to combine near and far offset travel time analysis (Landrø and Stammeijer 2004) to estimate velocity and thickness changes simultaneously. Hatchell et al. and Røste et al. suggested in 2005 using a factor (R) relating the relative velocity change (dv/v) to the relative thickness change (dz/z; displacement)

$$R = -\frac{dv/v}{dz/z} \tag{19.9}$$

Hatchell et al. found that this factor varies between 1 and 5, and is normally less for the reservoir rock than for the overburden rocks. Laboratory measurements (Holt et al. 2008 and Bathija et al. 2009) show that the R-factor strongly depends on the stress state of the rock and the stress path, and that it typically decreases with increasing axial stress. For sandstones and clays it is common to establish empirical relationships between seismic P-wave velocity (v) and porosity (ϕ). These relations are often of the simple linear form:

$$v = a\phi + b \tag{19.10}$$

where a and b are empirical parameters. If a rock is stretched (or compressed), a corresponding change in porosity will occur. It is important to emphasise that Eq. (19.10) is simplified and does not include changes in grain contact stiffness or changes in crack density. Assuming that the lateral extent of a reservoir is large compared to its thickness, it is reasonable to assume a uniaxial strain condition as sketched in Fig. 19.17.

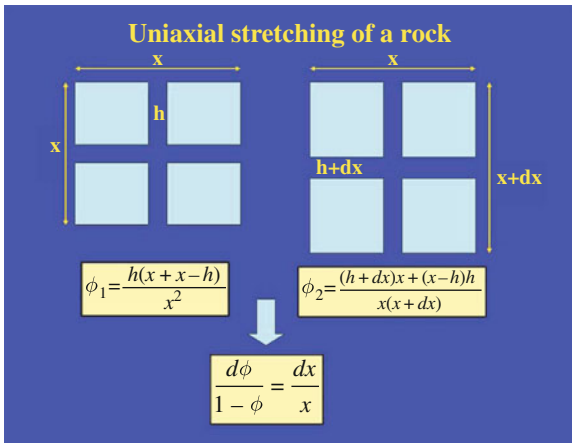

Fig. 19.17 Cartoon showing the effect of increased porosity due to stretching of a rock sample

From simple geometrical considerations we see that the relation between the thickness change and the corresponding porosity change is:

$$\frac{dz}{z} = \frac{d\phi}{1-\phi} \tag{19.11}$$

In the isotropic case (assuming that the rock is stretched in all three directions):

$$\frac{dz}{z} = \frac{d\phi}{3(1-\phi)} \tag{19.12}$$

Inserting Eqs. (19.10) and (19.11) into Eq. (19.9) we obtain an explicit expression for the dilation factor R:

$$R = 1 - \frac{a+b}{v} \tag{19.13}$$

which is valid only for the uniaxial case and assuming that velocity is only porosity dependent.

Using Eq. (19.12) instead of (19.11) gives a similar equation for the isotropic case. The relation between the measured time shift and the velocity and thickness changes is given as (Landrø and Stammeijer 2004):

$$\begin{aligned}\frac{dT}{T} &= -\frac{dv}{v} + \frac{dz}{z} = (1+R)\frac{dz}{z} \\ &= -\left(\frac{1+R}{R}\right)\frac{dv}{v}\end{aligned} \tag{19.14}$$

From Eq. (19.14) it is evident that we can estimate either the thickness change or the velocity change if the R-factor is known. Inserting Eq. (19.13) into (19.14) yields

$$\frac{dz}{z} = \left(\frac{v}{2v-a-b}\right)\frac{dT}{T} = S\frac{dT}{T} \tag{19.15}$$

where S is the strain-timestrain (by timestrain we simply mean the relative stretch of traveltime within the layer) ratio representing how much the relative stretch (or compaction) is for a given measured relative time shift. If the velocity-depth trend is known and the empirical parameters a and b are known we can estimate $S(z)$. As a simple example we use $v = v_0 + kz$, where $v_0 = 1500$ m/s and $k = 0.5$. Furthermore, if we use the empirical relationship obtained by Han et al. (1986) for shaly sandstones we find that

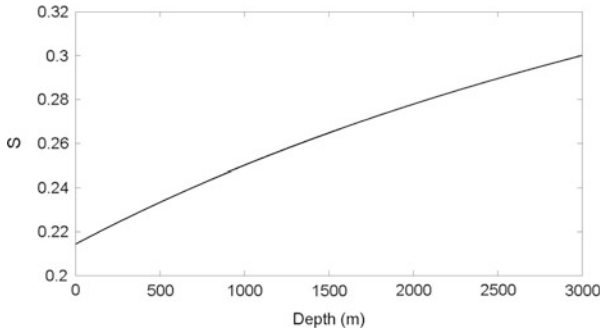

Fig. 19.18 Sensitivity ratio (S) between relative stretching (strain) and measured relative time shift (dT/T) assuming a = -7000 m/s and b = 3000 m/s in equation 19.15, and that v = 1500 +0.5z

a = -7000 m/s and b = 3000 m/s, roughly. Using these values in equation 19.15 gives a sensitivity that increases slightly with increasing depth, as shown in Fig. 19.18. However, it is important to stress that the above assumption of uniaxial stretching of the overburden rocks might be too simple, especially for reservoirs of finite lateral extent. In such cases, the vertical and horizontal strains will have opposite sign, as shown by Tempone et al. (2009; Fig. 19.19) and Tempone (2011). This means that the net volumetric strain is typically less than the vertical and horizontal strains, as shown in Fig. 19.20. If the basement layer (150 m below the reservoir) is rigid, the geomechanical modelling shows that the volumetric strains near to the surface are negative while those closer to the reservoir are positive. Furthermore, we observe from Fig. 19.20 that the volumetric strain below the reservoir is positive and significant.

According to Geertsma's model (Fjær et al. 2008) the volumetric strain will be close to zero for the rocks surrounding the reservoir. This means that the porosity change in the overburden is zero, and thus for depletion the vertical stress decrease will be accompanied by a horizontal stress increase (equal to half the vertical stress change). For an inflated reservoir, the opposite situation will apply. Therefore, it seems very likely that the mono-causal porosity model discussed above does not capture the physics correctly. Stress changes are probably as important as porosity changes, and in many cases stress might be the dominant effect. Geertsma's model is a simplification, and especially heterogeneities and reservoir geometry will change the overburden stress path.

Both the overburden and reservoir rocks are exposed to anisotropic stress changes, leading to anisotropic velocity changes. How to couple geomechanical modelling to time-lapse seismic data is still a research topic, focusing on a variety of methods. As the accuracy and repeatability level of time-lapse seismic data improves, it is realistic to assume that this research area will become more important in the future.

19.8 Discrimination Between Pore Pressure and Saturation Effects

Although the main focus in most 4D seismic studies is to study fluid flow and detect bypassed oil pockets, the challenge of discriminating between pore pressure changes and fluid saturation changes occurs frequently. From rock physics we know that both effects influence the 4D seismic data. However, as can be seen from Fig. 19.8, the fluid pressure effects are not linked to the seismic parameters in the same way as the fluid saturation effects. This provides an opportunity to discriminate them, since we have different rock physics relations for the two cases. Some of the early attempts to perform this discrimination between pressure and saturation were presented by Tura and Lumley (1999) and Landrø (1999). In Landrø's method (2001) the rock physics relations (based on Gassmann and ultrasonic core measurements) are combined with simple AVO (amplitude versus offset) equations to obtain direct expressions for saturation changes and pressure changes. Necessary input to this algorithm is near and far offset amplitude changes estimated from the base and monitor 3D seismic cubes. This method was tested on a compartment from the Cook Formation at the Gullfaks Field. Figure 19.21 shows a seismic profile (west–east) through this compartment.

A significant amplitude change is observed for the top Cook interface (red solid line in the figure), both below and above the oil/water contact. The fact that this amplitude change extends beyond the oil/water contact is a strong indication that it cannot be solely related to fluid saturation changes, and a reasonable candidate is therefore pore pressure changes. Indeed, it was confirmed that the pore pressure had increased by 50–60 bars in this segment, meaning that the reservoir pressure is approaching fracture pressure. We also

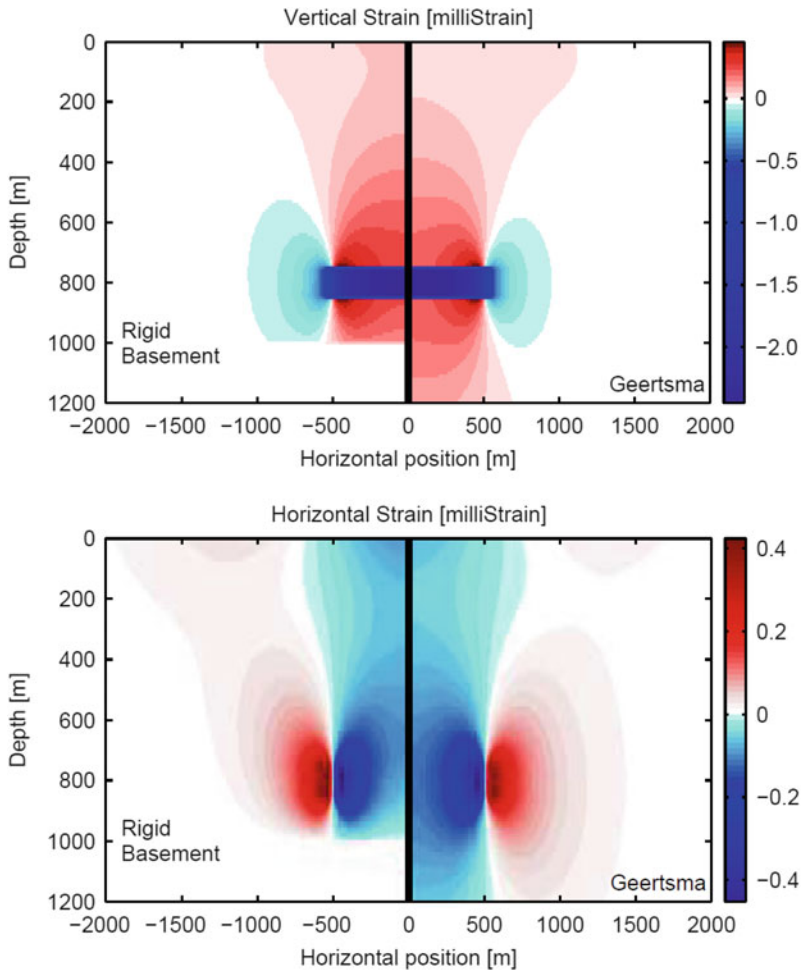

Fig. 19.19 Vertical strain (top) caused by a compacting reservoir assuming a rigid basement below the reservoir (left) and using Geertsma's solution (right). The reservoir extends from 750 to 850 m in depth and has a lateral extension of 1000 m. Corresponding results for the horizontal strain are shown in the bottom plot. (Source: Pamela Tempone's PhD thesis, NTNU, 2011 and SPE paper SPE-121081)

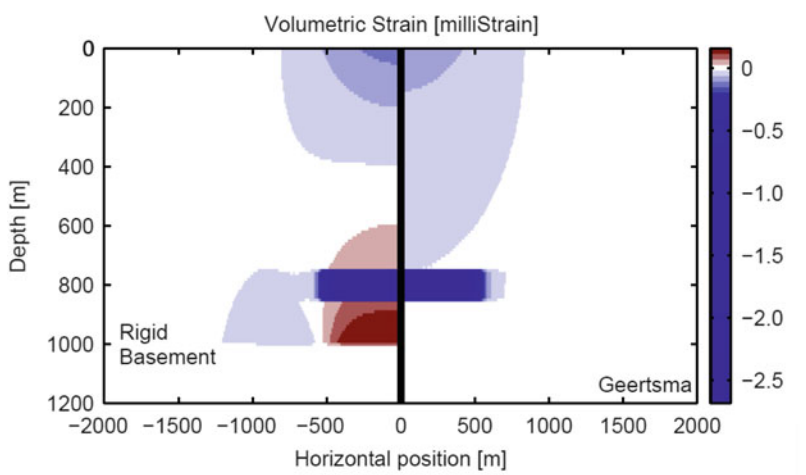

Fig. 19.20 Vertical strain caused by a compacting reservoir assuming a rigid basement (left), and using Geertsma's solution (right). (Source: Pamela Tempone's PhD thesis, NTNU, 2011 and SPE paper SPE-121081)

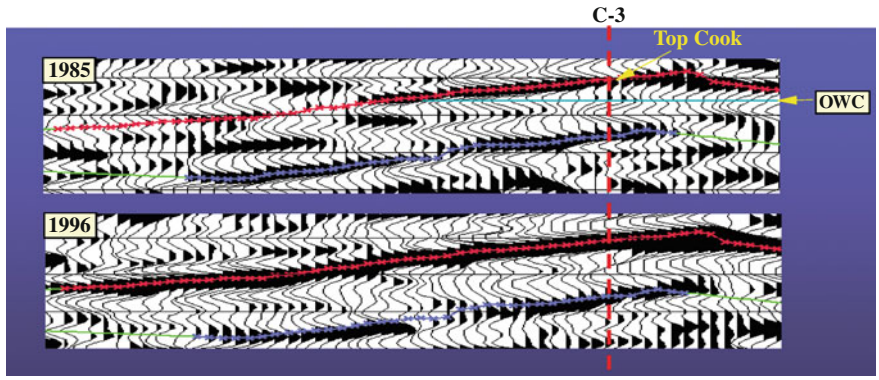

Fig. 19.21 Seismic section through the Cook Formation at Gullfaks. The *cyan solid line* indicates the original oil/water contact (marked OWC). Notice the significant amplitude change at *top* Cook between 1985 and 1996, and that the amplitude change extends beyond the OWC-level, a strong indication that the downflank amplitude change is caused by pore pressure changes

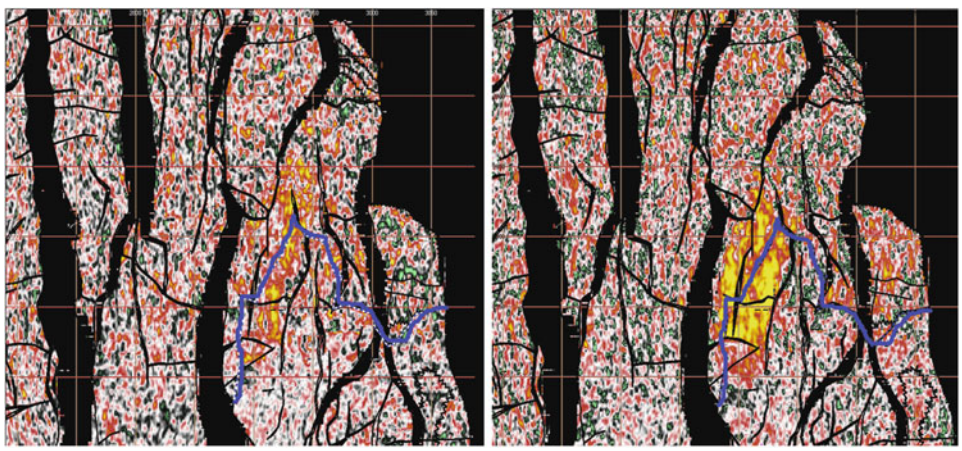

Fig. 19.22 Estimated fluid saturation changes (*left*) and pore pressure changes (*right*) based on 4D AVO analysis for the *top* Cook interface at Gullfaks. The *blue solid line* represents the original oil/water contact. Notice that the estimated pressure changes extend beyond this *blue line* to the west, and terminate at a fault to the east. *Yellow colours* indicate significant changes

observe from this figure that the base reservoir event (blue solid line) is shifted slightly downwards, by 2–3 ms. This slowdown is interpreted as a velocity drop caused by the pore pressure increase in the segment.

Figure 19.22 shows an attempt to discriminate between fluid saturation changes and pressure changes for this compartment using the method described in Landrø (2001). In 1996, 27% of the estimated recoverable reserves in this segment had been produced, so we know that some fluid saturation changes should be observable on the 4D seismic data.

From this figure we see that in the western part of the segment most of the estimated fluid saturation changes occur close to the oil/water contact. However, some scattered anomalies can be observed beyond the oil/water contact in the northern part of the segment. These anomalies are probably caused by inaccuracies in the algorithm or by limited repeatability of the time-lapse AVO data. The estimated pressure changes are more consistent with the fault pattern in the region, and it is likely that the pressure increase is confined between faults in almost all directions. Later time-lapse surveys show that the eastern fault in the figure was "opened" some years later.

19.9 Other Geophysical Monitoring Methods

Parts of this section are taken from "Future challenges and unexplored methods for 4D seismics", by Landrø, Recorder (2005).

Up to now, 4D seismic has proved to be the most effective way to monitor a producing reservoir. However, as discussed above, there are several severe limitations associated with time lapse seismic. One of them is that seismic reflection data is sensitive to acoustic impedance (velocity times density). Although 4D time shift can reveal changes in average velocity between two interfaces, an independent measurement of density changes would be a useful complement to conventional 4D seismic. The idea of actually measuring the mass change in a reservoir caused by hydrocarbon production has been around for quite some time. The limiting factor for gravimetric reservoir monitoring has been the repeatability (or accuracy) of the gravimeters. However, Sasagawa et al. (2003) demonstrated that improved accuracy can be achieved by using 3 coupled gravimeters placed on the seabed. This technical success led to a full field programme at the Troll Field, North Sea. Another successful field example was time-lapse gravity monitoring of an aquifer storage recovery project in Leyden, Colorado (Davis et al. 2005), essentially mapping water influx. Obviously, this technique is best suited for reservoirs where significant mass changes are likely to occur, such as water replacing gas. Shallow reservoirs are better suited than deep. The size of the reservoir is a crucial parameter, and a given minimum size is required in order to obtain observable effects. In quite another field, gravimetric measurements might help in monitoring volcanic activity by distinguishing between fluid movements and tectonic activity within an active volcano.

Around 2000 the hydrocarbon industry started to use electromagnetic methods for exploration. Statoil performed a large-scale research project that showed that it is possible to discriminate between hydrocarbon-filled and water-filled reservoirs from controlled source electromagnetic (CSEM) measurements. Since this breakthrough of CSEM surveys some years ago (Ellingsrud et al. 2002), this technique has mainly been used as an exploration tool, in order to discriminate between hydrocarbon-filled rocks and water-filled rocks. Field tests have shown that such data are indeed repeatable, so there should definitely be a potential for using repeated EM surveys to monitor a producing reservoir. So far, frequencies as low as 0.25 Hz (and even lower) are being used, and then the spatial resolution will be limited. However, as a complementary tool to conventional 4D seismic, 4D EM might be very useful. In many 4D projects it is hard to quantify the amount of saturation changes taking place within the reservoir, and time-lapse EM studies might be used to constrain such quantitative estimates of the saturation changes. Furthermore, unlike conventional 4D seismic which is both pressure and saturation sensitive, the EM technique is not very sensitive to pressure changes, so it may be a nice tool for separating between saturation and pressure changes.

In another paper, Johansen et al. (2005) show that the EM response over the Troll West gas province is significantly above the background noise level, see Fig. 19.23. If we use the deviation from a smooth response as a measure of the repeatability level, a relative amplitude variation of approximately 0.1–0.2 (measured in normalised EM amplitude units) is observed. Compared to the maximum signal observed at the crest of the field (2.75) this corresponds to a repeatability level of 4–7%, which is very good compared to conventional time-lapse seismic. This means it is realistic to assume that time-lapse EM data can provide very accurate low-resolution (in x-y plane) constraints on the saturation changes observed on 4D seismic data. Recently, Mittet et al. (2005) showed that depth migration of low frequency EM data may be used to enhance the vertical resolution. In a field data example, the vertical resolution achieved by this type of migration is maybe of the order of a few hundred metres. The EM sensitivity is determined by the reservoir thickness times the resistivity, underlining the fact that both reservoir thickness and reservoir resistivity are crucial parameters for 4D CSEM. This means that the resolution issue with the active EM method is steadily improving, and such improvements will of course increase the value of repeated CSEM data as a complement to conventional 4D seismic.

By using the so-called interferometric synthetic aperture radar principle obtained from orbiting satellites, an impressive accuracy can be attained in

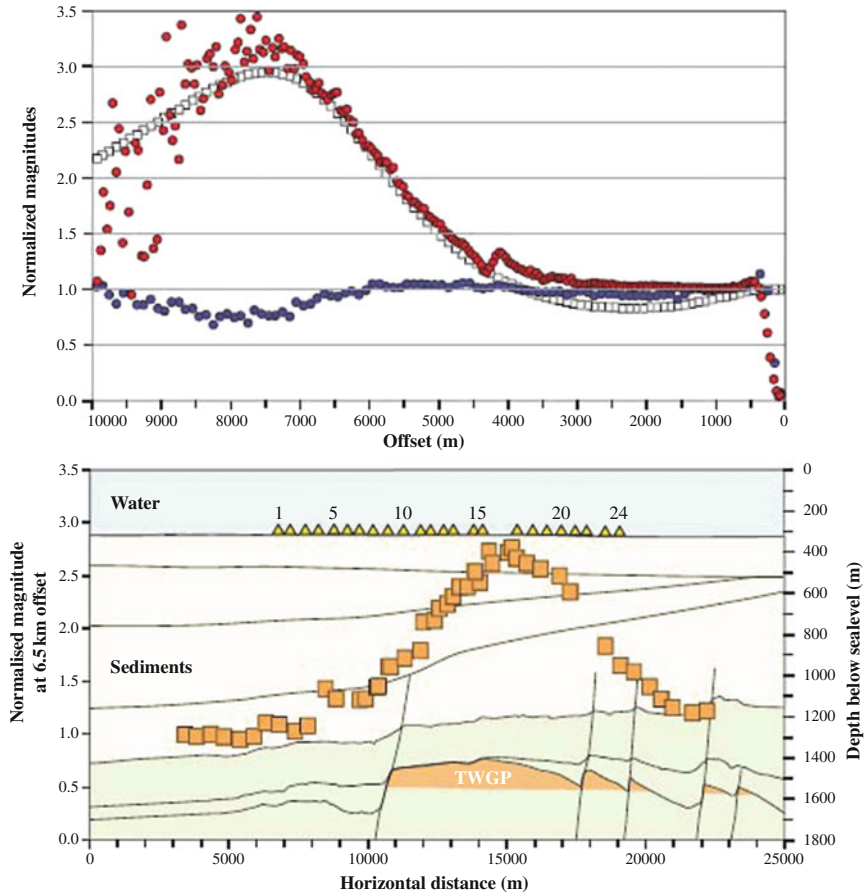

Fig. 19.23 Modelled (*open circles*) and measured (*red circles*) relative electrical field strength as a function of offset (*top*). The values are normalised to the response outside the reservoir (*blue circels*). *Bottom* figure shows relative values for a constant offset of 6.5 km along a profile, where the background shows the reservoir model. Notice that the relative signal increases by a factor of 3 above the thickest part of the reservoir. (Figure taken from Johansen et al. 2005)

measuring the distance to a specific location on the Earth's surface. By measuring the phase differences for a signal received from the same location for different calendar times, it is possible to measure the relative changes with even higher accuracy. By exploiting a sequence of satellite images, height changes can be monitored versus time. The satellites used for this purpose orbit at approximately 800 km.

Several examples of monitoring movements of the surface above a producing hydrocarbon reservoir have been reported, though there are of course limitations to the detail of information such images can provide for reservoir management. The obvious link to the reservoir is to use geomechanical modelling to tie the movements at the surface to subsurface movements. For seismic purposes, such a geomechanical approach can be used to obtain improved velocity models in a more sophisticated way. If you need to adjust your geomechanical model to obtain correspondence between observed surface subsidence and reservoir compaction, then this adjusted geomechanical model can be used to distinguish between overburden rocks with high and low stiffness for instance, which again can be translated into macro-variations of the overburden velocities. The deeper the reservoir, the lower the frequency (less vertical resolution) of the surface imprint of the reservoir changes, thus this method can not be used directly to identify small pockets of undrained hydrocarbons. However, it can be used as a complementary tool for time-lapse seismic since it can provide valuable information on the low frequency spatial signal (slowly varying in both horizontal and vertical directions) of reservoir compaction.

19.10 CO_2 Monitoring

This text is taken from the paper "Quantitative Seismic Monitoring Methods" by Landrø (2008), in ERCIM News 74, pp. 16–17:

Interest in CO_2 injection, both for storage and as a tertiary recovery method for increased hydrocarbon production, has grown significantly over the last decade. Statoil has stored approximately 10 million tons of CO_2 in the Utsira Formation at the Sleipner Field, and several similar projects are now being launched worldwide. At NTNU our focus has been to develop geophysical methods to monitor the CO_2-injection process, and particularly to try to quantify the volume injected directly from geophysical data.

One way to improve our understanding of how the CO_2 flows in a porous rock is to perform small-scale flooding experiments on long core samples. Such experiments involve injecting various fluids in the end of a 30–40 cm long core (Fig. 19.24). An example of such a flooding experiment and corresponding X-ray images for various flooding patterns is shown in Fig. 19.24. By measuring acoustic velocities as the flooding experiment is conducted, these experiments can be used to establish a link between pore-scale CO_2-injection and time-lapse seismic on the field scale.

Figure 19.25 shows an example of how CO_2 influenced the seismic data over time. By combining 4D travel time and amplitude changes, we have

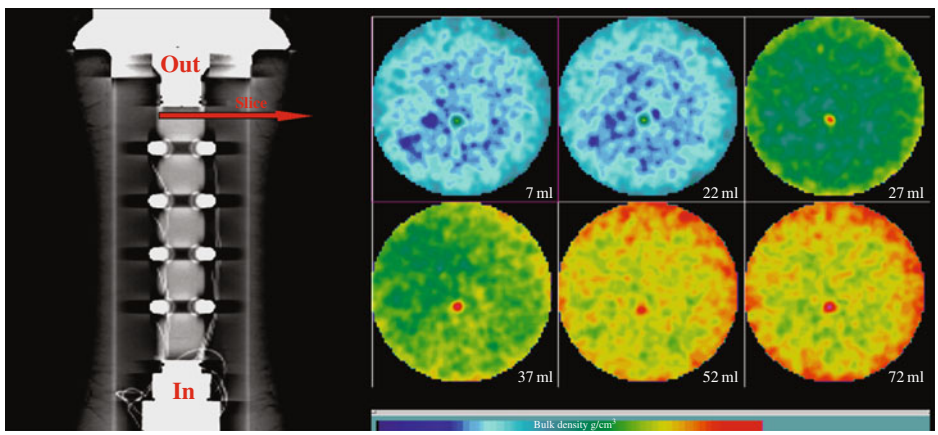

Fig. 19.24 Long core (*left*) showing the location for the X-ray cross-section (*red arrow*). Water injection is 50 g/l. To the *right*: X-ray density maps of a core slice: 6 time steps during the injection process. (From Marsala and Landrø, EAGE extended abstracts 2005)

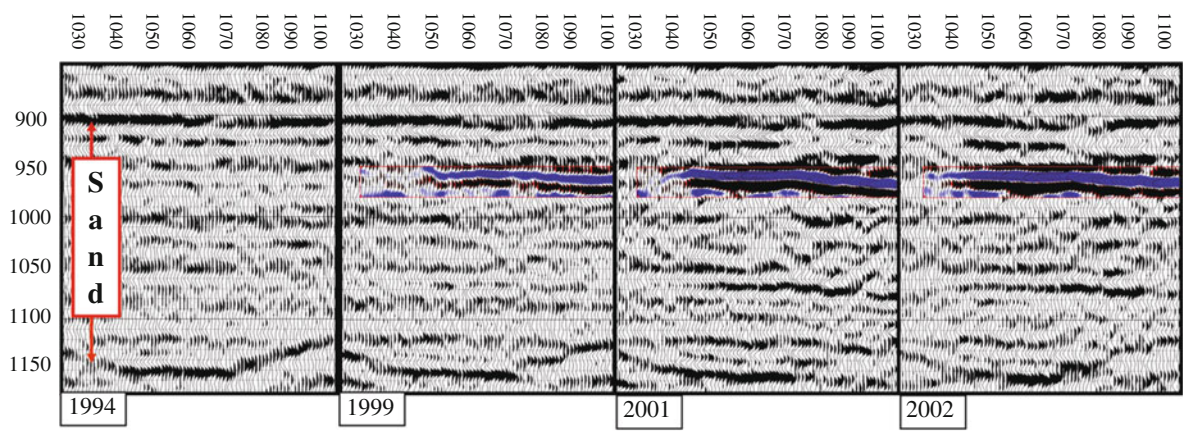

Fig. 19.25 Time-lapse seismic data showing monitoring of the CO_2 injection at Sleipner. The strong amplitude increase (shown in *blue*) is interpreted as a thin CO_2 layer. (Printed with permission from Statoil)

developed methods to estimate the thickness of CO_2 layers, which makes it possible to estimate volumes. Another key parameter is CO_2 saturation, which can be estimated using rock physics measurements and models. Although the precision in both 4D seismic methods and rock physics is increasing, there is no doubt that precise estimates are hard to achieve, and therefore we need to improve existing methods and learn how to combine several methods in order to decrease the uncertainties associated with these monitoring methods.

19.11 Time-lapse Refraction Methods

Refraction methods are among the oldest methods in seismic exploration. The term refraction is not unique or precise. According to Sheriff (2002) it has two meanings, first to change direction (following Snell's law) and second to involve head waves. In this chapter I will use a relaxed interpretation which means that the term includes head waves, diving waves and reflections close to critical angle. Maybe long offset time-lapse seismic is more correct. Within petroleum geophysics, one of the first proposals to exploit this type of data for 4D purposes was presented by Landrø et al. 2004. It was suggested that 4D refraction analysis could be of potential benefit for carbonate reservoirs. The basic condition for generation of head waves is that the incidence angle of a seismic wave is larger than the critical angle θ_C:

$$\sin\theta_C = \frac{v_1}{v_2} \tag{19.16}$$

where v_1 and v_2 denote the velocity above and below the top reservoir (or the target) interface. It is evident from this equation that there has to be a velocity increase in order to create head waves for incidence angles greater than the critical angle. This is also one of the major limitations for this method: it does not work for interfaces where the velocity contrast is weak or decreasing. Another weakness of the method is that it relies on dominantly horizontal wave propagation, and therefore it is most robust for detecting velocity changes that are laterally extensive. Small, localised 4D anomalies are better resolved by using conventional 4D reflection methods. However, in a situation where the velocity changes caused by production are small (less than a few per cent), the time lapse refraction method might be attractive. A simple synthetic example based on a six-layer model is shown in Fig. 19.26, where we observe that the major difference signal occurs for offsets close to the critical offset. In this case, the velocities of the cap rock and the reservoir layer are 2000 and 2500 m/s, respectively. For the monitor survey, we have assumed that the reservoir velocity increases to 2600 m/s. The differences observed in Fig. 19.26 are caused by a combination

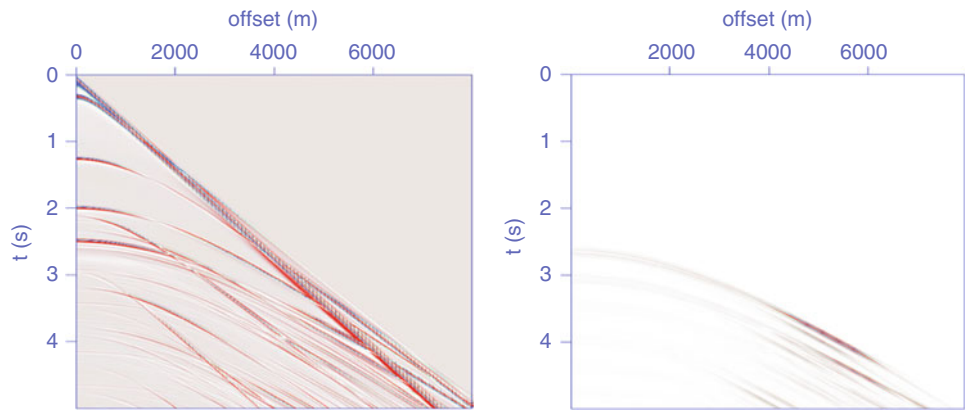

Fig. 19.26 Synthetic 4D refraction example: Modelled base survey (*left*) for a 6-layer model, and the corresponding difference section, assuming that the velocity of the reservoir layer is changed from 2500 m/s to 2600 m/s. The largest changes occur close to the critical offset around 5–6 km. The vertical axis is from 0 to 5 seconds, and the horizontal offset axis is from 0 to 8 km. (Figure from Landrø et al. 2004)

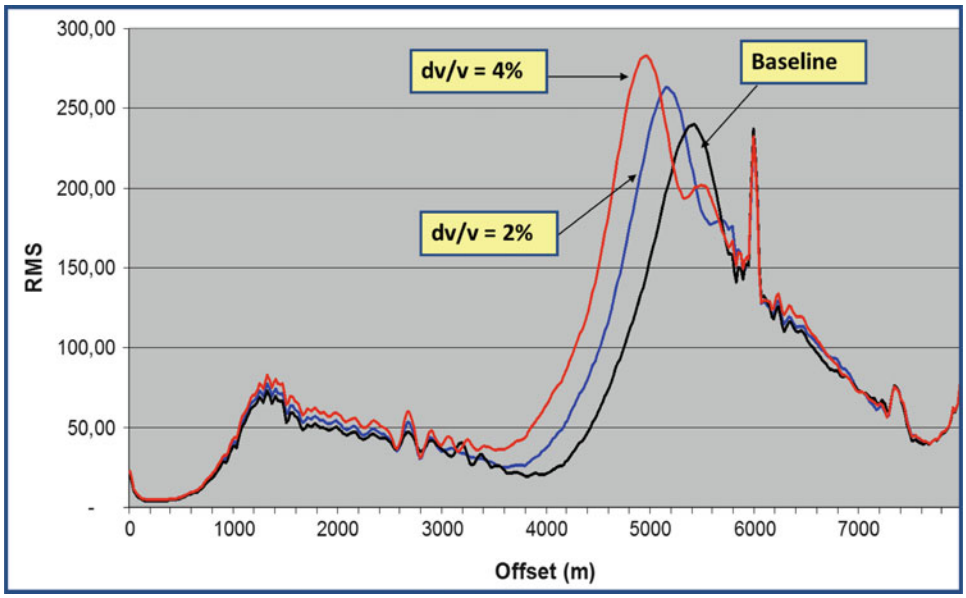

Fig. 19.27 RMS (Root Mean Square, after fk-filtering) analysis of the synthetic data example demonstrating that the amplitude increase close to critical offset is moving towards shorter offsets when the velocity of the reservoir layer is slightly decreased (2% and 4% reduction, respectively)

of travel time and amplitude changes. We notice that the differences at zero offset are negligible, as expected.

A reliable and simple way to detect the change in critical angle is to use a windowed RMS (Root Mean Square) technique, as shown in Fig. 19.27. A clear shift in the RMS-curve is observed assuming small velocity changes (2 and 4%). An fk-filter has been applied to the data in order to enhance the refracted signal in Fig. 19.27. Is it likely that we can observe similar effects for field data? One concern is that long offset seismic data is less repeatable and that noise created by multiple reflections and refractions in the water layer (see Landrø 2007) will distort a clean and precise picking of such offset shifts.

An example using the LoFS (Life of Field Seismic) acquired at the Valhall Field demonstrates that it is possible (Fig. 19.28). We clearly see an offset shift similar to that for the synthetic case. We observe changes between LoFS survey number 1 and 6 and that this change continues when compared to LoFS survey number 8. The interpretation of these shifts is, however, not as simple as for the synthetic case, since the Valhall field is compacting. The compaction at the reservoir level causes stretching of the overburden shale, and some of the offset change is attributed to this effect and some to saturation and pressure changes within the reservoir layer, as discussed by Zadeh et al. 2011.

In the second example from Valhall we observe no changes between survey 1 and 6, followed by a significant offset shift between survey number 6 and 8 (Fig. 19.29). This example clearly demonstrates the advantage of acquiring several frequent surveys: it is possible to monitor detailed reservoir changes that might occur over a half year interval. When a permanent array is installed at a field, each survey is relatively cheap since a single source vessel is sufficient to acquire a repeat survey.

Another application of time lapse refraction is to detect changes in shallow sediments. One such example is sketched in Fig. 19.30, where an underground blow-out (from well 2/4-14, the same as shown in Fig. 19.3), causes gas to be trapped in a thin sand layer. In this case, the most robust 4D refraction attribute is the time shift. The time shifts attributed to the velocity reduction are observed from conventional site survey data acquired before and after the blow-out, as shown in Fig. 19.31. For comparison, a corresponding gather outside the gas-filled area is shown, clearly demonstrating no time shifts in this case. For site survey data, the amplitude repeatability is not of the same quality as for normal seismic data. There are several potential causes for this lower

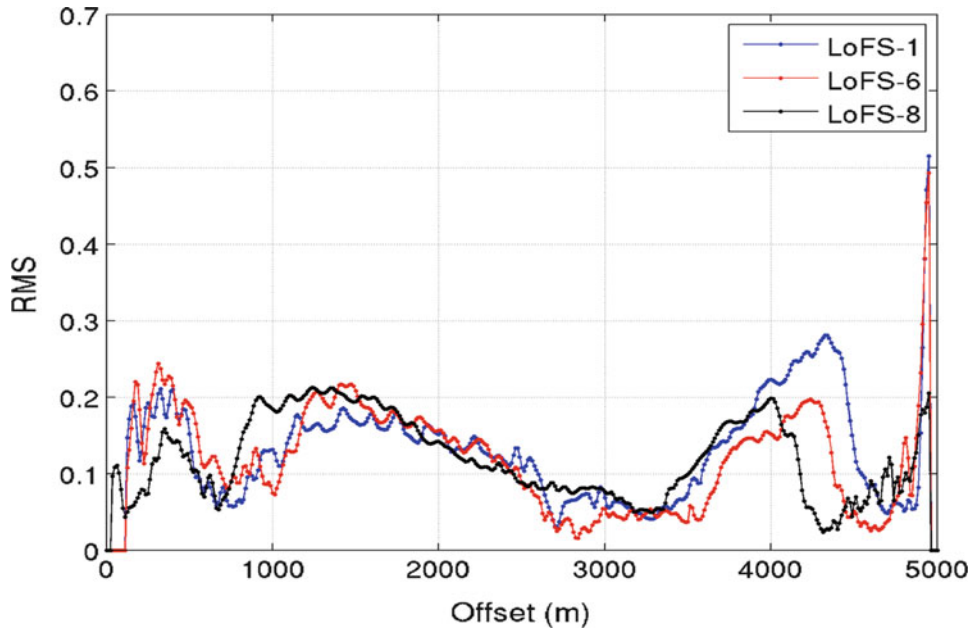

Fig. 19.28 Field data example using LoFS data from Valhall. We observe a clear shift towards shorter offsets for the interpreted amplitude increase close to critical offset (4000–4500 m). (Figure from Zadeh et al. 2011)

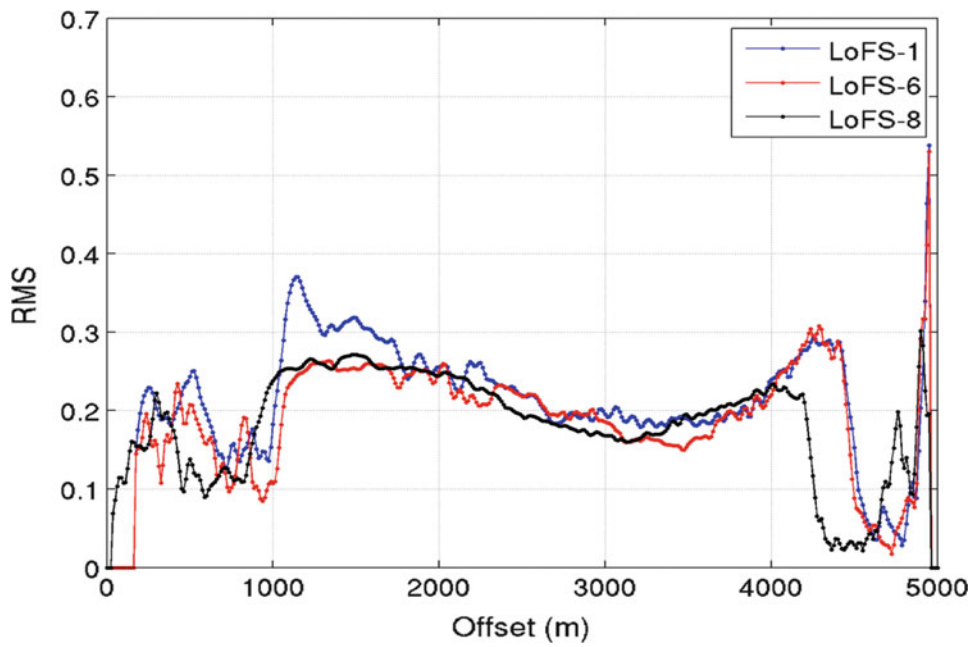

Fig. 19.29 Example 2 using Valhall LoFS data: Here we observe no changes between LoFS1 and LoFS6, followed by a significant change of approximately 300 m for the LoFS8 survey. (From Zadeh et al. 2011)

repeatability level: smaller source arrays, more variability in streamer sensitivity and shallower towing depth (causing more noise in rough weather) are some of them.

Figure 19.32 shows a systematic estimation of time shifts using offsets ranging from 1000 m to 1150 m (Zadeh and Landrø 2011). Despite some scatter in the time shift estimates, we observe a clear increase close

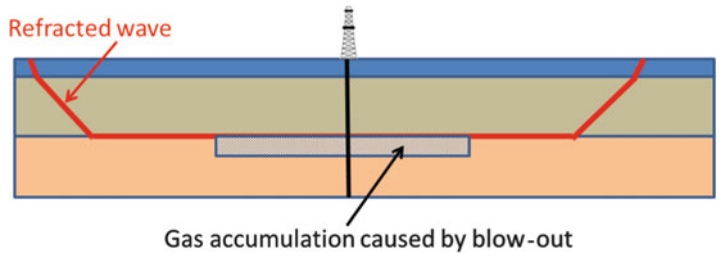

Fig. 19.30 Schematic plot showing how 4D refraction analysis can be used to detect shallow gas leakage

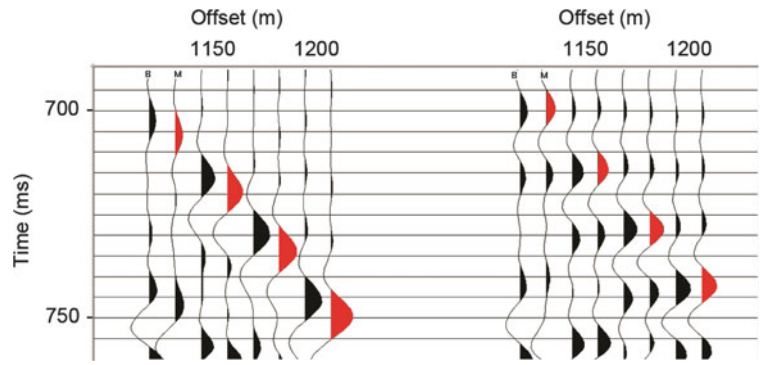

Fig. 19.31 Observed time shift for the refracted wave close to the blow-out well (*left*) and similar display far away from the well (*right*). Black traces (B=Base) are before blow-out and red (M=Monitor) traces after. Typical time shifts within the gas anomaly are of the order of 3-4 ms. (Zadeh and Landrø 2011)

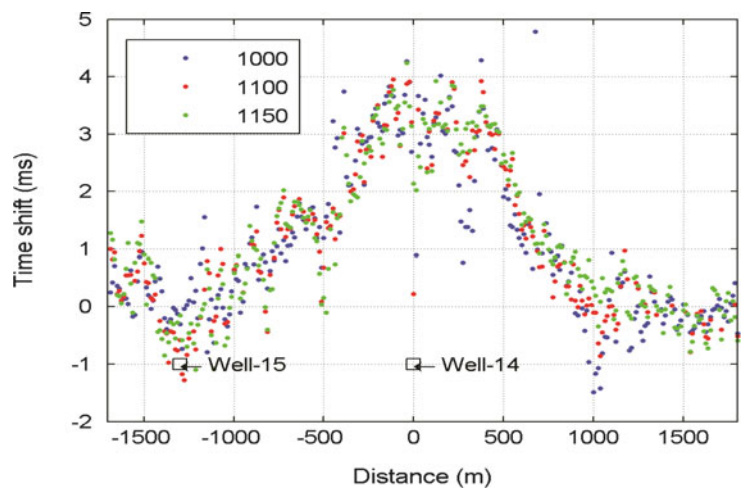

Fig. 19.32 Estimated refraction time shifts for three offsets close to the blow-out well (14): A positive time shift of up to 4 ms is observed. (From Zadeh and Landrø 2011)

to the blow-out well (14). The maximum time shift is 4 ms. The thickness of the gas-filled sand layer is approximately 10 m.

A third example of time lapse refraction is shown in Fig. 19.33, where time shifts are observed close to a region where steam is injected into a heavy oil

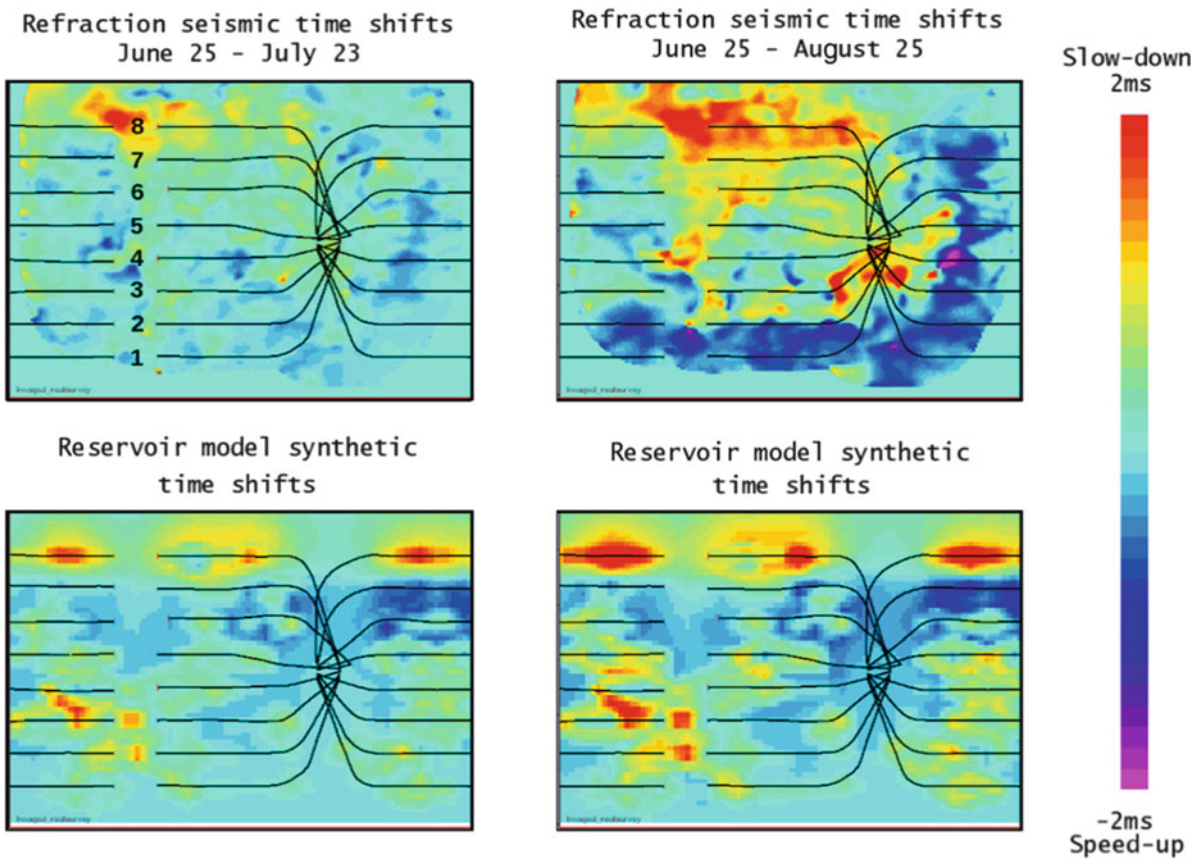

Fig. 19.33 Time lapse refraction example from Peace River heavy oil field in Alberta. Significant velocity reduction caused by steam injection into row 8. (Figure from Hansteen et al. 2010)

reservoir in Alberta, Canada (Hansteen et al. 2010). When steam is injected, the stiffness of the rock is reduced, leading to a velocity decrease. This velocity decrease leads to a corresponding increase in time shift, as observed in Fig. 19.33.

Hilbich (2010) uses time-lapse refraction seismic tomography to study seasonal changes in the ground ice in the Alps. He concludes that the method is capable of detecting temporal changes in alpine permafrost and can identify ground ice degradation. A major strength of the method is according to Hilbich the high vertical resolution potential and the ability to discriminate phase changes between frozen and unfrozen material over time. A significant limitation is the low penetration depth due to strong velocity contrasts between the active layer and the permafrost table.

Presently, time lapse refraction is not well established as a 4D technique. The few examples presented so far illustrate that the technique has a potential. One weakness is that it is hard to map the time lapse anomalies precisely in depth. Fortunately, full wave form inversion techniques have developed significantly over the last decade (Virieux and Operto 2009, Sirgue et al. 2009). A few examples of this technique have also been presented for 4D applications (Routh et al. 2009). Therefore, there is hope that time lapse refraction methods might develop into a more precise and accurate technique. Despite this lack of more advanced analysis methods, it is important to underline that if 4D refraction is used as a tool for detecting shallow gas leakage, the important issue is to detect and locate approximately where the leakage occurs. Detailed and accurate mapping of the 4D anomaly is not crucial. Should more accurate mapping be required, this may be done across the located area by conventional reflection survey.

19.12 Future Aspects

The most important issue for further improvement of the 4D seismic method, is to improve the repeatability. Advances in both seismic acquisition and 4D processing will contribute to this process. As sketched in Fig. 19.13, it is expected that this will be less pronounced than in the past decade. However, it is still a crucial issue, and even minor improvements might mean a lot for the value of a 4D seismic study. Further improvements in repeatability will probably involve issues like source stability, source positioning, shot time interval, better handling of various noise sources. Maybe in the future we will see vessels towing a superdense grid of sensors, in order to obtain perfect repositioning of the receiver positions.

Another direction to improve 4D studies could be to constrain the time-lapse seismic information by other types of information, such as geomechanical modelling, time-lapse EM, gravimetric data or innovative rock physics measurements.

Our understanding of the relation between changes in the subsurface stress field and the seismic parameters is still limited, and research within this specific area will be crucial to advance the 4D. New analysis methods like long offset 4D, might be used as a complementary technique or as an alternative method where conventional 4D analysis has limited success. However, long offset 4D is limited to reservoirs where the velocity increases from the cap rock to the reservoir rock.

The link between reservoir simulation (fluid flow simulation) and time-lapse seismic will continue to be developed. As computer resources increase, the feasibility of a joint inversion exploiting both reservoir simulation and time-lapse seismic data in the same subsurface model will increase. Despite extra computing power, it is reasonable to expect that the non-uniqueness problem (several scenarios will fit the same datasets) will require that the number of Earth models is constrained by models predicting the distribution of rock physical properties based on sedimentology, diagenesis and structural geology.

Acknowledgments Statoil is acknowledged for permission to use and present their data. The Research Council of Norway is acknowledged for financial support to the ROSE (Rock Seismic) project at NTNU. Lasse Amundsen, Lars Pedersen, Lars Kristian Strønen, Per Digranes, Eilert Hilde, Odd Arve Solheim, Ivar Brevik, Paul Hatchell, Peter Wills, Jan Stammeijer, Thomas Røste, Rodney Calvert, Alexey Stovas, Lyubov Skopintseva, Andreas Evensen, Amir Ghaderi, Dag O. Larsen, Kenneth Duffaut, Jens Olav Paulsen, Jerome Guilbot, Olav Barkved, Jan Kommedal, Per Gunnar Folstad, Helene Veire, Erling Fjær, Pamela Tempone, Rune Martin Holt, Ola Eiken, Torkjell Stenvold, Fredrik Hansteen and Alberto Marsala are all thanked for co-operation and discussions.

Further Reading

Amundsen, L. and Landrø, M. December 2007. 4D seismic – Status and future challenges, Part II. GeoExpro, 54–58.

Barkved, O. 2004. Continuous seismic monitoring. 74th Annual International Meeting, The Society of Exploration Geophysicists, 2537–2540.

Barkved, O., Buer, K., Halleland, K.B., Kjelstadli, R., Kleppan, T. and Kristiansen, T. 2003. 4D seismic response of primary production and waste injection at the Valhall field. 65th Meeting. European Association of Geoscientists and Engineers, Extended Abstracts, A22.

Barkved, O.I. and Kristiansen, T. 2005. Seismic time-lapse effects and stress changes: Examples from a compacting reservoir. The Leading Edge 24, 1244.

Bathija, A.P., Batzle, M.L. and Prasad, M. 2009. An experimental study of the dilation factor. Geophysics 74, E181–E191.

Calvert, R. 2005. Insights and methods for 4D reservoir monitoring and characterization, EAGE/SEG Distinguished Instructor Short Course 8.

Christensen, N.I. and Wang, H.F. 1985. The influence of pore pressure and confining pressure on dynamic elastic properties of Berea sandstone. Geophysics 50, 207–213.

Davis, K., Li, Y., Batzle, M. and Reynolds, B. 2005. Time-lapse gravity monitoring of an aquifer storage recovery project in Leyden, Colorado. 75th Annual International Meeting. The Society of Exploration Geophysicists, GM1.4.

Eiken, O., Zumberge, M., Stenvold, T., Sasagawa, G. and Nooen, S. 2004. Gravimetric monitoring of gas production from the Troll Field. 74th Annual International Meeting. The Society of Exploration Geophysicists, 2243–2246.

Ellingsrud, S., Eidesmo, T., Johansen, S., Sinha, M.C., MacGregor, L.M. and Constable, S. 2002. Remote sensing of hydrocarbon layers by seabed logging (SBL): Results from a cruise offshore Angola. The Leading Edge 21(10), 972–982.

Fjær, E., Holt, R.M., Horsrud, P., Raaen, A.M. and Risnes, R. 2008. Petroleum Related Rock Mechanics, 2nd edition. pp. 402-409. Elsevier, ISBN 978-0-444-50260-5.

Foldstad, P.G., Andorsen, K., Kjørsvik, I. and Landrø, M. 2005. Simulation of 4D seismic signal with noise – Illustrated by WAG injection on the Ula Field. 75th Annual International Meeting. The Society of Exploration Geophysicists, TL2.7.

Furre, A-K., Munkvold, F.R. and Nordby, L.H. 2003. Improving reservoir understanding using time-lapse seismic at the Heidrun Field, 65th Meeting. European Association of Geoscientists and Engineers, A20.

Gassmann, F. 1951. Über die elastizität poroser medien. Vierteljahrsschrift der Naturforchenden Gesellschaft in Zürich 96, 1–23.

Gosselin, O., Aanonsen, S.I., Aavatsmark, I., Cominelli, A., Gonard, R., Kolasinski, M., Ferdinandi, F., Kovacic, L. and Neylon, K. 2003. History matching using time-lapse seismic (HUTS), SPE paper 84464.

Guilbot, J. and Smith, B. 2002. 4-D constrained depth conversion for reservoir compaction estimation: Application to Ekofisk Field. The Leading Edge 21(3), 302–308.

Han, D., Nur, A. and Morgan, D. 1986. Effects of porosity and clay content on wave velocities in sandstones. Geophysics, **51**, 2093–2107.

Hansteen, F., Wills, P.B., Hornman, K. and Jin, L. 2010. Time-lapse refraction seismic monitoring. 80th Annual International Meeting. Society of Exploration Geophysicis, 4170-4174.

Hatchell, P.J. and Bourne, S.J. 2005. Rocks under strain: Strain-induced time-lapse time shifts are observed for depleting reservoirs. The Leading Edge 24, 1222–1225.

Hatchell, P.J., Kawar, R.S. and Savitski, A.A. 2005. Integrating 4D seismic, geomechanics and reservoir simulation in the Valhall oil field. 67th Meeting. European Association of Geoscientists and Engineers, C012.

Hilbich, C. 2010. Time-lapse refraction seismic tomography for the detection of ground ice degradation. The Cryosphere 4, 243–259.

Holt, R.M., Fjær, E., Nes, O.-M. and Stenebråten, J.F. 2008. Strain sensitivity of wave velocities in sediments and sedimentary rocks. ARMA (American Rock Mechanics Association; conference paper) 08-291, 1-8.

Johansen, S.E., Amundsen, H.E.F., Røsten, T., Ellingsrud, S., Eidesmo, T. and Bhuyian, A.H. 2005. Subsurface hydrocarbons detected by electromagnetic sounding. First Break 23, 31–36.

Kommedal, J.H., Barkved, O.I. and Howe, D.J. 2004. Initial experience operating a permanent 4D seabed array for reservoir monitoring at Valhall. 74th Annual International Meeting. The Society of Exploration Geophysicists, 2239–2242.

Koster, K., Gabriels, P., Hartung, M., Verbeek, J., Deinum, G. and Staples, R. 2000. Time-lapse seismic surveys in the North Sea and their business impact. The Leading Edge 19 (03), 286–293.

Kragh, E. and Christie, P. 2002. Seismic repeatability, normalized rms, and predictability. The Leading Edge 21, 640–647.

Landrø, M. 1999. Repeatability issues of 3-D VSP data. Geophysics 64, 1673–1679.

Landrø, M. 2001. Discrimination between pressure and fluid saturation changes from time lapse seismic data. Geophysics 66(3), 836–844.

Landrø, M. 2002. Uncertainties in quantitative time-lapse seismic analysis. Geophysical Prospecting 50, 527–538.

Landrø, M. 2007. Attenuation of seismic water-column noise – tested on seismic data from the Grane field. Geophysics 72, V87–V95.

Landrø, M. 2008. The effect of noise generated by previous shots on seismic reflection data. Geophysics 73, Q9–Q17.

Landrø, M., Digranes, P. and Strønen, L.K. 2001. Mapping reservoir pressure and saturation changes using seismic methods – Possibilities and limitations. First Break 19, 671–677.

Landrø, M., Digranes, P. and Strønen, L.K. 2002. Pressure effects on seismic data – Possibilities and limitations. Paper presented at the NPF biennual conference, Kristiansand, Norway, 11–13 March, 2002.

Landrø, M., Digranes, P. and Strønen, L.K. 2005. Pressure depletion measured by time-lapse VSP. The Leading Edge 24, 1226–1232 (December issue).

Landrø, M. and Duffaut, K. 2004. V_p–V_s ratio versus effective pressure and rock consolidation – A comparison between rock models and time-lapse AVO studies. 74th Annual International Meeting. The Society of Exploration Geophysicists, 1519–1522.

Landrø, M., Nguyen, A.K. and Mehdizadeh, H. 2004. Time lapse refraction seismic – A tool for monitoring carbonate fields? 74th Annual International Meeting. The Society of Exploration Geophysicists, 2295–2298.

Landrø, M., Nguyen, A.K. and Zadeh, M.H. 2004. Time lapse refraction seismic – a tool for monitoring carbonate fields? 74th Annual International Meeting. The Society of Exploration Geophysicists, 2295–2298.

Landrø, M. and Skopintseva, L. 2008. Potential improvements in reservoir monitoring using permanent seismic receiver arrays. The Leading Edge 27, 1638–1645.

Landrø, M., Solheim, O.A., Hilde, E., Ekren, B.O. and Strønen, L.K. 1999. The Gullfaks 4D seismic study. Petroleum Geoscience 5, 213–226.

Landrø, M. and Stammeijer, J. 2004. Quantitative estimation of compaction and velocity changes using 4D impedance and traveltime changes. Geophysics 69(4), 949–957.

Landrø, M., Veire, H.H., Duffaut, K. and Najjar, N. 2003. Discrimination between pressure and fluid saturation changes from marine multicomponent time-lapse seismic data. Geophysics 68, 1592–1599.

Larsen, D. and Lie, A. 1990. Monitoring an underground flow by shallow seismic data: A case study. SEG Expanded Abstracts 9, 201 pp.

MacLeod, M., Hanson, R.A., Bell, C.R. and McHugo, S. 1999. The Alba Field ocean bottom cable survey: Impact on development. The Leading Edge 18, 1306–1312.

Mavko, G., Mukerji, T. and Dvorkin, J. 1998. The Rock Physics Handbook. Cambridge University Press, Cambridge, ISBN 0521 62068 6, 147–161.

Mehdi Zadeh, H., Landrø, M., Mythen, B.A., Vedanti, N. and Srivastava, R. 2005. Time lapse seismic analysis using long offset PS data. 75th Annual International Meeting. The Society of Exploration Geophysicists, TL3.7.

Mindlin, R.D. 1949. Compliance of elastic bodies in contact. Journal of Applied Mechanics 16, 259–268.

Nes, O.M., Holt, R.M. and Fjær, E. 2000. The reliability of core data as input to seismic reservoir monitoring studies. SPE 65180.

Osdal, B., Husby, O., Aronsen, H.A., Chen, N. and Alsos, T. 2006. Mapping the fluid front and pressure buildup using 4D data on Norne Field. The Leading Edge 25, 1134–1141.

Parr, R., Marsh, J. and Griffin, T. 2000. Interpretation and integration of 4-D results into reservoir management, Schiehallion Field, UKCS. 70th Annual International Meeting. The Society of Exploration Geophysicists, 1464–1467.

Rogno, H., Duffaut, K., Furre, A.K., Eide, A.L. and Kvamme, L. 1999. Integration, quantification and dynamic updating – Experiences from the Statfjord 4-D case. 69th Annual International Meeting. The Society of Exploration Geophysicists, 2051–2054.

Røste, T., Stovas, A. and Landrø, M. 2005. Estimation of layer thickness and velocity changes using 4D prestack seismic data. 67th Meeting. European Association of Geoscientists and Engineers, C010.

Routh, P., Palacharla, G., Chikichew, I. and Lazaratos, S. 2012. Full wavefield inversion of time-lapse data for improved imaging and reservoir characterization. SEG Expanded Abstracts, 1–6.

Sasagawa, G.S., Crawford, W., Eiken, O., Nooner, S., Stenvold, T. and Zumberge, M. 2003. A new sea-floor gravimeter. Geophysics 68, 544–553.

Settari, A. 2002. Reservoir compaction. SPE paper **76805**, 62–69.

Sheriff, R.E. 2002. Encyclopedic dictionary of applied geophysics. Society of Exploration Geophysicists. ISBN 0-931830-47-8.

Sirgue, L., Barkved, O.I., Van Gestel, J.P., Askim, O.J. and Kommedal, J. H. 2009. 3D waveform inversion on Valhall wide-azimuth OBC. EAGE expanded abstracts, U038.

Stovas, A. and Landrø, M. 2004. Optimal use of PP and PS time-lapse stacks for fluid pressure discrimination. Geophysical Prospecting, European Association of Geoscientists and Engineers 52, 301–312.

Tempone, P. 2011. Effects of reservoir compaction on seismic and gravity monitoring. PhD thesis, NTNU, 2011:6, ISBN 978-82-471-2519-9.

Tempone, P., Landrø, M., Fjær, E. and Inoue, N. 2009. Effects on time-lapse seismic of a hard rock layer beneath a compacting reservoir (SPE-121081).

Tura, A. and Lumley, D.E. 1999. Estimating pressure and saturation changes from time-lapse AVO data. 69th Annual International Meeting, The Society of Exploration Geophysicists, Expanded Abstracts, 1655–1658.

Tøndel, R. and Eiken, O. 2005. Pressure depletion observations from time-lapse seismic data at the Troll Field. 67th EAGE Meeting, Abstract, C037.

Vasco, D.W., Datta-Gupta, A., Behrens, R., Condon, P. and Rickett, J. 2004. Seismic imaging of reservoir flow properties: Time-lapse amplitude changes. Geophysics 69, 1425–1442.

Virieux, J and Operto, S., 2009. An overview of full-waveform inversion in exploration geophysics. Geophysics 74, WCC1-WCC26.

Watts, G.F.T., Jizba, D., Gawith, D.E. and Gutteridge, P. 1996. Reservoir monitoring of the Magnus Field through 4D time-lapse seismic analysis. Petroleum Geoscience 2, 361–372.

Zadeh, M.H. and Landrø, M. 2011. Monitoring a shallow subsurface gas flow by time lapse refraction analysis. Geophysics 76, O35–O43.

Zadeh, M.H., Landrø, M. and Barkved, O.I. 2011. Long-offset time-lapse seismic: Tested on the Valhall LoFS data. Geophysics 76, O1–O13.

Zimmer, M., Prasad, M. and Baggeroer, A.B. 2002. Pressure and porosity influences on V_p–V_s ratio in unconsolidated sands. The Leading Edge 21(2), 178–183.